INTERFACE STRENGTH OF PILES EMBEDDED IN FROZEN SOILS

Zuhao Jin

A thesis submitted to the Faculty of Graduate and Postdoctoral Studies
in partial fulfillment of the requirements for the degree of

MASTER OF APPLIED SCIENCE

in

Civil Engineering

Ottawa-Carleton Institute for Civil Engineering
University of Ottawa
Ottawa, Canada

ABSTRACT

In this study, the effect of normal stress acting on a model scale pile is determined experimentally. The minimum soil temperature was -5^{o}C.

Additional experiments were conducted to determine the adfreeze bond strength of an interface between the Cornwall sand and a galvanized steel plate. These tests were done using a conventional direct shear apparatus. In order to conduct interface tests under freezing temperatures, some modifications were made on the direct shear apparatus. In these experiments, three different normal stresses and three different water contents were used.

The present study was extended to investigate whether there was any agreement between the adfreeze strength measured in the present study and the adfreeze strength calculated from the pull-out tests by Villeneuve (2017).

ACKNOWLEDGMENTS

I wish to express my most sincere gratitude to my research supervisors, Dr. Julio Angel Infante Sedano and Dr. Erman Evgin, who have shepherded me throughout the research process with their knowledge, experience and encouragement. I learned a lot from Dr. Infante and Dr. Evgin, not only in the study, but also in my life. I really enjoyed the research experience with them. Without their help and guidance, I could not put the research and thesis together.

I also wish to extend my sincerest gratitude to Dr. Rayhani and Dr. Fall who served as the examination committee members.

I would also like to thank the geotechnical laboratory officer Mr. Jean Claude Cédestin and structural laboratory officer Dr. Muslim Majeed for their big help in the laboratory.

I would also like to thank the staff of the Faculty of Engineering at the University of Ottawa for their help, particularly to Leo Denner, Xiuhan Yang, Yunlong Liu, Joey Villeneuve, Dr. Zhu Fu, and Luc Cloutier.

It would not be possible for me to pursue my Master's degree without the emotional and financial support from my parents. Hereby, I express my sincere gratitude to them.

Thank you to all.

TABLE OF CONTENTS

LIST OF FIGURES

LIST OF TABLES

CHAPTER ONE

GENERAL INTRODUCTION

1.1 Problem Statement

There are many regions of the world where soils are permanently or seasonally frozen. The engineering behavior of soils in those regions is affected by thermo-hydro-mechanical (THM) processes. For example, below freezing temperatures, the mechanical properties of soil, such as stiffness and strength, can increase significantly. The amount of change in the mechanical behavior mostly depends on the amount of water in the soil, the soil density, the length of time under consideration, and the magnitude of the temperature (Andersland and Ladanyi, 1994). On the other hand, if the temperature of the frozen ground rises above zero Celsius, the soil will start thawing. As a result of increasing temperatures, the soil stiffness and its shear strength will decrease. In addition, the temperature difference in different sections of the ground would cause the flow of water from warmer areas to the colder areas in the ground. When this water freezes at the cold front, heaving takes place and results in considerable damage to engineering structures (Konrad and Morgenstern, 1984).

In order to minimize the adverse effects of the THM processes on foundation behavior, geotechnical engineers frequently use piles to support structures in frost susceptible environments.

The bearing capacity of a pile is the sum of shaft resistance and toe resistance. The shaft resistance of a pile in frozen soil is calculated by multiplying the adfreeze strength with the surface area of the pile shaft. The adfreeze strength is the maximum resistance of the soil-structure interface to shearing. The toe resistance is usually ignored because its development

requires a large amount of displacement unless the pile toe is supported by bedrock. Therefore, the adfreeze bond strength at the interface between a pile and the frozen soil is the main contributor to the bearing capacity of the pile foundations to transfer the load to the ground. So it is very important for engineers to know the adfreeze strength at the pile-soil interface to adequately design pile foundations in frozen soils.

In order to make use of solar energy, solar panels are used in Cornwall, Ontario in an open field. The solar panels are supported by piles. For the design purposes, technical information is needed on the behavior of these piles during freezing temperatures for both compressive loadings due to the weight of the panels and tensile loading caused by wind on the solar panels.

1.2 Objectives

The most important parameter in the calculation of pull-out resistance of a pile during tensile loading is the adfreeze bond strength between the soil and the pile shaft. The main objective of the present investigation is to determine the adfreeze bond strength of a pile installed in Cornwall sand. There are two types of experiments that can be conducted to determine the adfreeze bond strength. One of them is a pull-out test on a model scale pile. The other type of experiment is to use an interface apparatus to determine the adfreeze bond strength. It has been shown by Parameswaran (1978), Choi et al. (1977), and some other investigators that the magnitude of adfreeze bond strength is affected by the normal stress acting on the interface.

The objectives of the present investigation are as follows.

(i) To determine the confining pressure acting on the pile shaft during a freeze process using a laboratory experiment.

(ii) To measure the adfreeze bond strength of Cornwall Sand using interface testing method.

(iii) To obtain a relationship between adfreeze bond strength and water content of Cornwall sand using interface experiments.

(iv) To obtain a relationship between adfreeze bond strength and normal stress acting on the pile-soil interface.

(v) To compare the adfreeze bond strength obtained from interface tests with the adfreeze bond strength obtained from the pull-out tests which were done by Villeneuve (2017) and to see if they match.

(vi) To determine the changes in confining pressure acting on pile shaft due to warming permafrost.

1.3 Research Methodology

In order to determine the adfreeze bond strength at the interface between the Cornwall Sand and the pile shaft, two types of experiments were conducted. The first set of experiments was used to measure the soil confining pressure acting on a PVC tube representing the model scale pile. The confining pressure is generated first by dynamic compaction of soil. Subsequently, the hollow cylindrical soil sample which is contained between the PVC tube and the soil container was subjected to freezing temperatures causing changes in the

confining pressure. These tests were conducted in a freezer in the structural lab at the University of Ottawa.

The second set of experiments is used to measure directly the adfreeze bond strength of the interface between the Cornwall Sand and steel plates with similar surface roughness as the piles supporting the solar panels. The normal stresses used in these experiments were taken from the first set of experiments described in the previous paragraph. These adfreeze tests were conducted using the interface testing machine in the Geotechnical Lab at the University of Ottawa. To accomplish the objectives of the present investigation, the interface machine was modified to apply below zero temperatures on the soil samples.

1.4 Outline of Thesis

(i) Chapter 2 presents a literature review about frozen ground engineering and pile foundations in permafrost.

(ii) Chapter 3 presents the properties of Cornwall sand used in this study and the soil confining pressure acting on the pile shaft during freezing.

(iii) Chapter 4 presents the results of the soil-pile interface tests which were done to determine the adfreeze bond strength.

(iv) Chapter 5 presents a numerical analysis using finite element software PLAXIS to investigate the response of soil samples in cold room experiments to temperature changes.

(v) Chapter 6 presents the comparison of adfreeze bond strength determined by the pull-out tests of Villeneuve (2017) and the results of adfreeze tests of the present study.

(vi) Chapter 7 has the summary and conclusions of the present study.

CHAPTER TWO

LITERATURE REVIEW

2.1 Frozen Soils

For soils to be frozen, the ground temperature needs to be at least below 0^{o}C. However, the freezing temperature is influenced by many factors, such as pore water chemistry, confining pressure, soil mineraloly, etc. Frozen soils are found in many parts of the world. The term permafrost is used for soils when the ground temperature remains below zero at least two years. Distribution of permafrost in the North Hemisphere is shown in Figure 2.1. In the frozen soils, soil particles are fused together by ice so the strength of frozen soils is bigger than that of unfrozen soils (Andersland and Ladanyi, 2004).

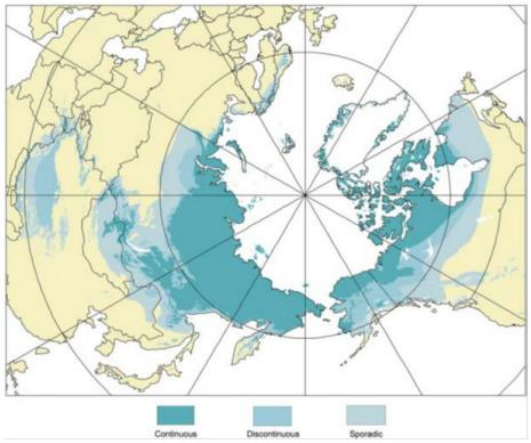

Figure 2.1 Permafrost in the Northern Hemisphere (Brown et al., 1998)

"Subsurface temperatures are influenced by soil thermal properties, air temperatures and ground cover" (Andersland and Ladanyi, 2004). Ground surface temperature varies with time. Local meteorological data is used to estimate the ground surface temperatures as shown in Equation 2.1.

$$T = T_m + T_a \sin \frac{2\pi t}{p} \qquad \text{Eq. 2.1}$$

where T is the ground surface temperature, T_m is the mean annual temperature, T_a is the surface temperature amplitude, t is the time and p is the period (Andersland and Ladanyi, 2004).

The active layer is the layer at the top part of the ground. It is in either a frozen state or an unfrozen state at different times in the year. Its thickness varies in different locations and depends on many factors, such as snow cover, local temperature and surface vegetation (Andersland and Ladanyi, 2004).

Frozen soils are composed of four phases, namely the soil particles, ice, liquid water and air. A simple power equation was given by Tice, Anderson, and Banin (1976) showing the relationship between unfrozen water content and temperature in frozen soils as shown in Equation 2.2

$$w_u = \alpha \theta^{\beta} \qquad \text{Eq. 2.2}$$

where w_u is the unfrozen water content, the symbols α and β are soil properties and θ is the temperature in degrees Celsius below 0^{o}C. In addition, if the soil contains dissolved salts in its pore water, which will result in a lower freezing point of water in the soil (Andersland and Ladanyi, 2004). An equation was given by Patterson and Smith (1983) for estimating the freezing temperature due to the salinity of a solution as shown in Equation 2.3.

$$T_n = T_i + \frac{S_n}{A(\frac{w_u}{w})} \qquad \text{Eq. 2.3}$$

where T_n is the freezing temperature, w_u is the unfrozen water content in soil which does not have dissolved salts and T_i is the corresponding temperature, S_n is the salinity of soil water, A equals to -17.04(g/1)/°C, w is the total water content including frozen and unfrozen water contents.

In cold regions, the effect of frost heave and thaw settlement can have a profound effect on the performance of engineering structures and they need to be considered in design.

2.2 Adfreeze Bond Strength

The sum of adhesive strength at the ice-pile interface and frictional strength at the soil-pile interface is called the adfreeze strength (Parameswaran, 1978). Since 1930s, engineers have measured adfreeze bond strength, but the data measured was not detailed enough to develop a satisfactory design method for pile foundations in frozen soils (Parameswaran, 1978). In real life applications, there are many forces acting on piles embedded in frozen soils. Figure 2.2 is a schematic of a pile acted upon by various forces. Parameswaran (1978) stated that the inequality described in Eq. 2.4 should be met for pile-supported structures in permafrost

$$P + \tau_h A_h + \tau_d A_d + \tau_f A_f > L \qquad \text{Eq. 2.4}$$

"where P is the end bearing capacity of the pile; τ_f is the adfreeze strength at the pile-soil interface; A_f is the pile-soil interfacial area in the permafrost zone; τ_d is the frictional drag stress (i.e., skin friction) between the pile and the unfrozen soil (if present) in the active

layer; A_d is the pile-soil interfacial area in this zone; L is the structural load, and a combination of several live loads such as seismic, wind, construction loading, and thermal expansion and contraction; τ_h is the stress due to frost heave in the frozen active layer; and A_h is the pile-soil interfacial area in the frozen active layer" (Parameswaran,1978). Parameswaran (1978) calls the adhesive bond "adfreeze bond". In the present study, the added effect of the adhesive bond strength and the frictional strength together are called adfreeze bond strength.

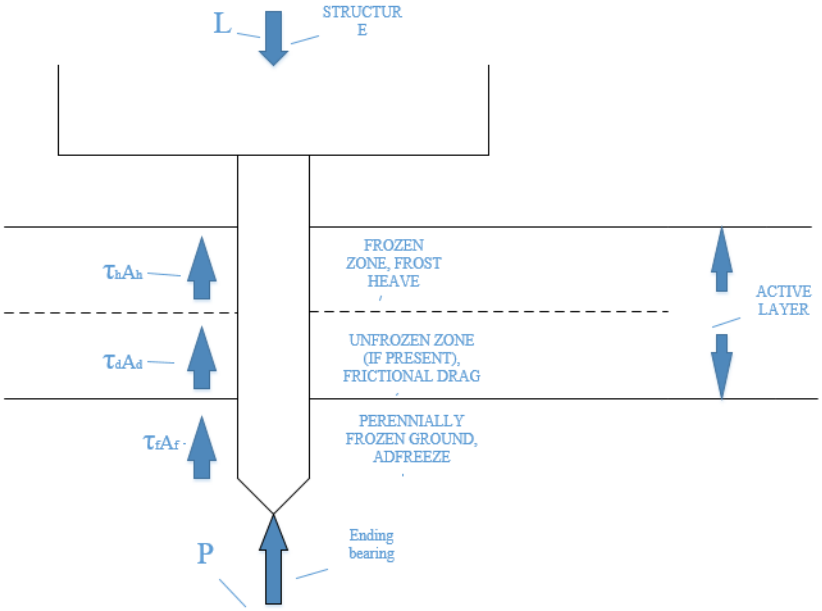

Figure 2.2 A schematic of a pile subjected to various forces in frozen soils (Parameswaran, 1978)

2.3 Temperature Effect on Adfreeze Bond Strength

Ground temperature has a major effect on ice strength and the percentage of ice content in frozen soils. In general, when the temperature decreases, the strength of frozen soils increases. The brittleness of the frozen soil will also increase with decreasing temperatures

below the freezing temperature. After a brittle failure, the frozen soil strength drops drastically (Sayles and Haines 1974; Haynes and Karalius 1977; Haynes 1978).

When frozen soil is thawing, the ice in the soil will melt and become liquid water. The structures built on thawing soil will settle due to consolidation. An equation for predicting thaw settlement is given by Crory (1973) as shown below.

$$\frac{\Delta H}{H_f} = 1 - \frac{\rho_{df}}{\rho_{d,th}} \qquad \text{Eq. 2.5}$$

where ρ_{df} and $\rho_{d,th}$ are the dry densities of frozen and unfrozen soils, respectively. H_f is the thickness of frozen soil. ΔH is the thickness difference before and after soil settlement. Equation 2.5 is a fast way to predict the potential thaw settlement without the need to run experiments in the lab (Andersland and Ladanyi, 2004). In addition to settlement, excess pore water pressures generated by faster soil thawing rates will reduce soil shear strengths (Andersland and Ladanyi, 2004). Therefore, undesirable engineering problems may happen.

2.4 Frost Protection and Thermal Insulation

Adfreeze bond strength is dependent on temperature. For the safety concerns of a foundation, the bottom of the foundation should be extended to the frost free area to protect the foundation from frost heave forces (Andersland and Ladanyi, 2004). Insulation can restrict the heat flow from one side to the other (Andersland and Ladanyi, 2004). Pile foundations are usually built below the critical isotherm (0°C) to protect the foundations from suffering frost penetration (Farouki 1992). Adamson, Claesson, and Eftring (1973) used the temperature of -1°C as the critical isotherm because some unfrozen water may still exist at that temperature. Moisture resistant membranes can be used to protect the insulation

materials from absorbing moisture (Andersland and Ladanyi, 2004). In addition, vapor diffusion and acids in the soil are also very important factors that need to be considered when using insulation materials (Andersland and Ladanyi, 2004).

2.5 Types of piles in frozen soils

In practice, there are many types of pile foundations in permafrost, such as timber piles, steel piles, concrete piles (Andersland and Anderson, 1978). Engineers have designed different kinds of pile sections to obtain higher pile capacity (Heydinger, 1987). For example, "protruding spikes are driven into timber piles and steel pieces are welded onto steel piles to obtain higher pile capacity" (Andersland and Alwahhab 1983; Crory 1966), thus, "failure will tend to occur in frozen soil rather than the pile" (Heydinger, 1987). By using corrugated piles, adequate pile adhesion can be attained to increase bearing capacity (Heydinger, 1987).

To keep permafrost in a low temperature, insulated piles are commonly used to prevent heat transfer from buildings to the pile foundations (Phukan 1980; 1985).

2.6 Pile installation methods in frozen soils

Both pile installation method and pile material will affect the adfreeze strength (Parameswaran, 1978, 1979, 1986; Weaver and Morgenstern, 1981 a and b). "The best conditions for pile installation are when the soils are fine-grained, the ice content of the soil is low, and the permafrost temperature is high although those are not the ideal conditions for adfreeze strength at the soil-pile interface"(Heydinger, 1987). Engineers install steel H-piles and open-ended piles in permafrost by sonic hammers (Ladanyi 1983; Nottingham and

Christopherson 1983; Phukan 1985). In addition, “It is impossible to drive piles in frozen gravels and cobbles without using pilot holes” (Heydinger, 1987).

If the diameter of the holes is larger than that of the piles, materials such as cement, slurry, sand and soil need to be backfilled between the pile and the wall of the hole (Heydinger, 1987). In practice, engineers also use artificial refrigerant to freeze ground quickly when it is necessary (Andersland and Ladanyi, 2004).

2.7 Design of piles in frozen soils

There are many factors that engineers must consider when designing pile foundations in frozen soils, such as applied load, adfreeze strength, allowable settlements, frost heave and so on. By using direct shear test machine in a cold room environment, Choi (2014) performed tests to determine the shear strength of two different frozen soils. These results were compared with the adfreeze bond strength of an interface between the same soil and a metal plate. The ratio between the adfreeze bond strength of the interface and the shear strength of the frozen soil was labeled as a coefficient r_s . Choi (2014) conducted experiments at different temperatures using pile materials with different surface roughness. He recommended that the coefficient r_s determined by experiments can be used in the design of pile foundations in frozen soils (Choi, 2014). There are two ways to determine the magnitude of the adfreeze bond strength (Choi, 2014). One of them is to shear the interface between the frozen soil and pile material. The other method is to multiply the frozen soil shear strength with the coefficient r_s mentioned above to obtain the adfreeze bond strength. The second method has been used by many investigators such as Sanger, 1969; Linell and Lobaca, 1980; Weaver and Morgenstern, 1981; Fang, 1991; and Bowles, 1996. The

magnitude and direction of the forces acting on piles are different in summer and winter months (Choi, 2014). Figure 2.3 shows the forces acting on pile foundations in frozen soils in summer and winter months (Choi et al. 2014 with reference to Phukan 1985).

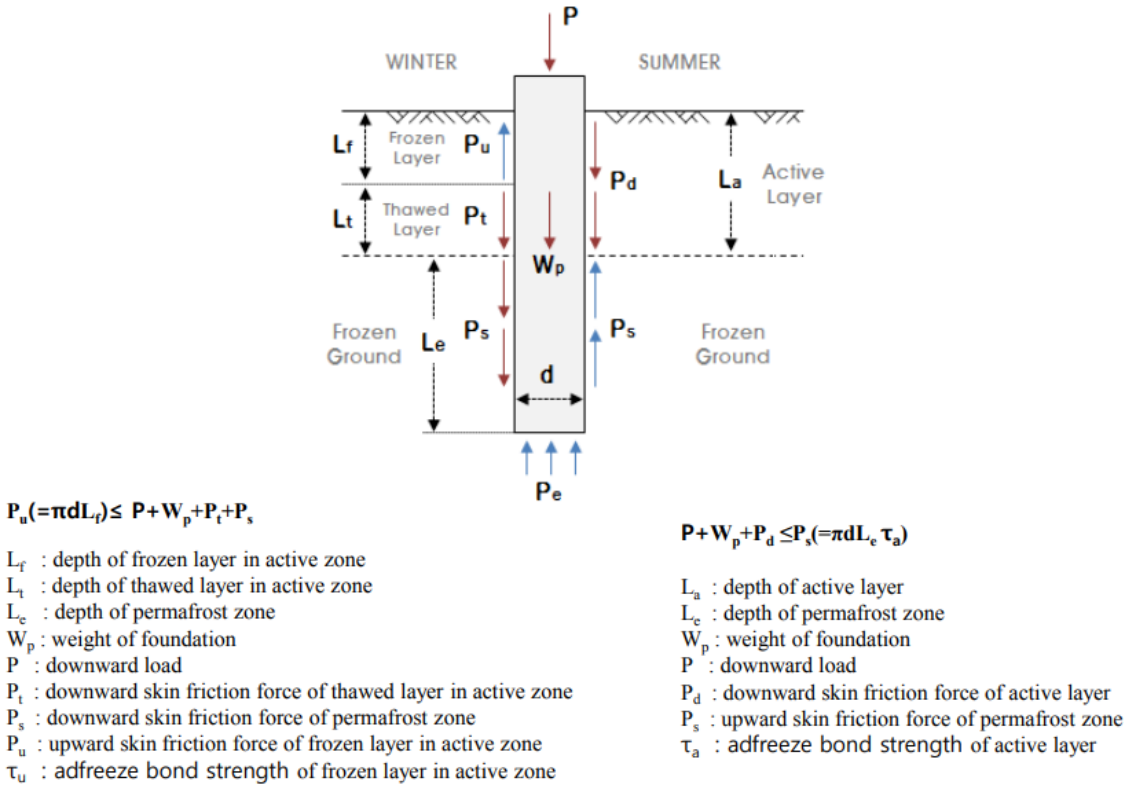

Figure 2.3 Forces acting on piles in frozen soils in summer and winter months (From Choi et al. 2014 with reference to Phukan, 1985)

Choi (2014) conducted experiments using an interface between Joomoonjin Sand and aluminum to determine the adfreeze bond strength. Table 2.1 is part of the test results of adfreeze bond strength. This table shows that the relationship between normal stress and adfreeze bond strength is not linear.

Table 2.1 Part of the test results of adfreeze bond strength (Choi, 2014)

Freezing Temperature (℃)	Normal stress (kPa)	Adfreeze bond strength (kPa)
-5	100	665
-5	200	816
-5	300	915

2.8 Frost heave

Frost heave is caused by ice formation in the soil. The direction of frost heave is upward. The magnitude of frost heave forces depends mainly on many factors such as soil properties, freezing rate, water supply, pile materials, soil temperature (Andersland and Ladanyi, 2004). Dalmatov's equation (Tsytovich, 1959) for estimating the magnitude of frost heave forces is shown below.

$$F = Lh_a(\mathrm{c} - 0.5bT_m) \qquad \text{Eq. 2.6}$$

where F is the frost heave force (kgf), L is the circumference of the foundation (cm), h_a is the depth of the frozen area (cm), T_m is the minimum soil temperature in degrees Celsius，b and c are experimental parameters. In addition, "soil creep will result in relaxation of stress which will decrease the magnitude of frost heave force" (Andersland and Ladanyi, 2004).

2.9 Creep and Failure at the Soil-Pile Interface

Creep is a time-dependent deformation under constant load. There are three stages of creep which are primary, secondary and tertiary creep during which time the creep rate is decreasing, constant and increasing, respectively. The secondary creep and tertiary creep

may not develop if the applied stress on the soil is lower than the long-term strength of frozen soil (Andersland and Ladanyi, 2004).

Andersland and Ladanyi (2004) stated that "Both the magnitude of applied stress and temperature will affect the shape of creep curves. For ice-saturated sands in medium-density to high-density under low stress conditions, the soils will only be in primary creep period. For ice-rich silts and clays, they will only display primary creep and secondary creep. Under high stress conditions, the frozen soils may exhibit tertiary creep directly and may fail in a very short time after loading, the high stress is called the short-term strength of the frozen soils".

Ladanyi (1972) developed a failure criterion shown in Equation 2.7:

$$t_f \dot{\varepsilon}_{\min} = \varepsilon_f \qquad \text{Eq. 2.7}$$

where t_f is the failure time, $\dot{\varepsilon}_{\min}$ is the minimum creep rate, ε_f is the total failure strain.

Andersland and Ladanyi (2004) found that if confining pressure increases, total failure strain ε_f will increase and if confining pressure decreases and the strain rates increase, total failure strain ε_f will decrease dramatically. In addition, if temperature decreases, ε_f will decrease.

2.10 Pile foundations in warming permafrost

Permafrost is commonly found in the Northern Hemisphere and some other parts of the world, especially in mountainous areas. Climate change has a profound effect on the

engineering behavior of permafrost. The air temperature has been on the rise due to increased emission of carbon dioxide from the use of fossil fuel. As a result, the permafrost temperature has also been increasing. The engineering properties of geomaterials in frozen state, which include strength, deformation properties and seepage characteristics, are highly dependent on the level of temperature. In the extreme case, when the air temperature goes above $0^{o}C$ for an extended period of time, the permafrost starts thawing from the ground surface downward. Many structures in permafrost areas are supported by pile foundations. The bearing capacity of piles in permafrost relies on the adfreeze bond strength. When the permafrost is warming, adfreeze bond strength at the pile-soil interface will decrease. This change in temperature will cause load carrying capacity of pile foundations to decrease. In addition, piles will also settle more due to soil consolidation which will cause additional problems for the structures supported by the pile foundations. The problems caused by settlement become worse if the amount of settlement is different at different parts of the building. For these reasons, it is essential for engineers to know how the adfreeze bond strength will change as a function of temperature and the creep behavior of piles in warming permafrost. With this knowledge, it might be possible to take corresponding safety measures to protect the structures from collapsing in warming permafrost.

In this section, the results of one of the most recent experimental research found in the literature are presented. Aldaeef and Rayhani (2017) conducted an experimental study on adfreeze strength and creep behavior of soil-structure interfaces. The soil used in their experiments was poorly graded sand. The maximum dry density of the poorly graded sand was $1.85 g/cm^3$ and the corresponding gravimetric water content was 10%. The pile material used in the experiment was structural steel plates. The steel plates used in the experiments

were 90mm long and 90mm wide. Figure 2.4 shows the modified components of the direct shear box. Thermocouples were used to monitor the temperature of the steel-soil interface in the experiments.

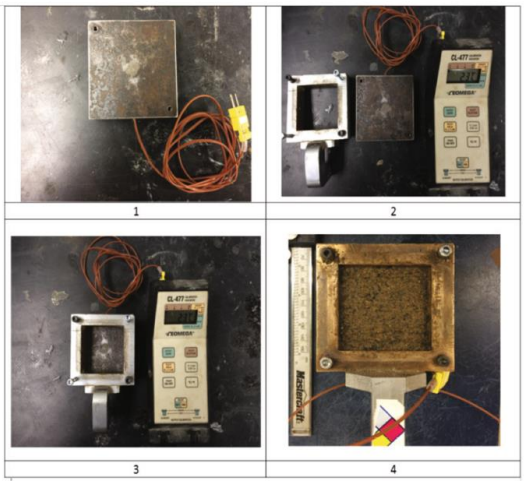

Figure 2.4 Modified direct shear box (Aldaeef and Rayhani, 2017)

2.10.1 Adfreeze bond strength tests of Aldaeef and Rayhani (2017)

This experimental work by Aldaeef and Rayhani (2017) was done in a walk-in cold room. In these experiments, the upper part of the shear box contained the soil and it remained stationary during the tests. The lower part of the shear box contained the steel plate and it moved horizontally at a constant rate to shear the steel-soil interface. Vertical load was applied on the soil sample to simulate the confining pressure acting on pile shaft in the field (Aldaeef and Rayhani, 2017). A load cell was used to measure the tangential force acting on the steel-soil interface. Labview software was used to take the horizontal and vertical displacement readings and record them.

In the experiments of Aldaeef and Rayhani (2017), the bulk density of the poorly graded sand was 2060 kg/m^3 and the corresponding water content was 13.5%. The freezing process

started after the normal load was applied on the sample to simulate the field condition. The system was frozen for 24 hours before shearing the interface. The horizontal displacement rate of the lower shear box was 0.00208 mm/min during the shearing process. Six temperature conditions were used during experiments which were -10^{o}C, -5^{o}C, -4^{o}C, -3^{o}C, -1.5^{o}C and +22^{o}C to investigate the temperature effect on the adfreeze bond strength. The normal stresses applied on the soil samples were 25kPa, 50kPa and 100kPa at each temperature (Aldaeef and Rayhani 2017).

The relationship between shear stress and shear displacement are shown in Figures 2.5 a, b and c. When the normal stress was kept constant, adfreeze strength decreased with an increase in temperature (Aldaeef and Rayhani 2017). These results indicate that, when the temperature in the permafrost increases, the bearing capacity of pile foundations will decrease (Aldaeef and Rayhani 2017).

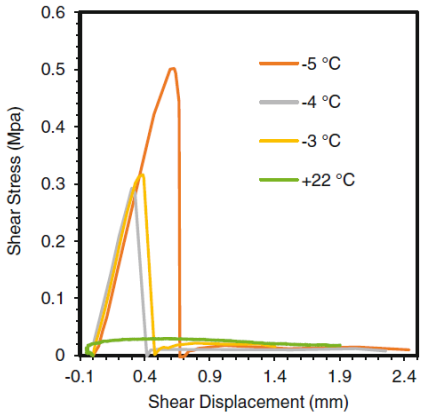

(a) The relationship between shear stress and shear displacement at 25kPa normal stress

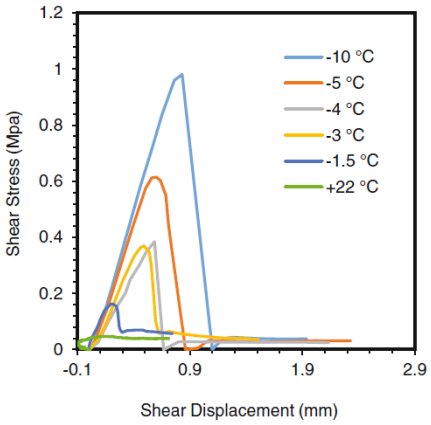

(b) The relationship between shear stress and shear displacement at 50kPa normal stress

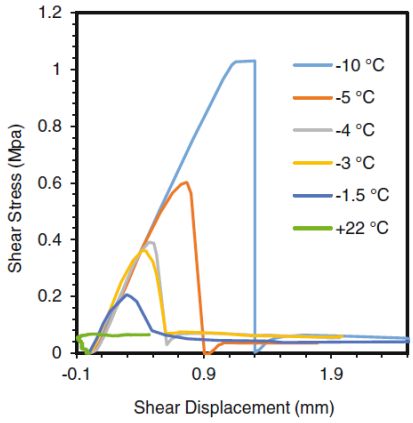

(c) The relationship between shear stress and shear displacement at 100kPa normal stress

Figure 2.5 Effects of temperature and normal stress on adfreeze strength (Aldaeef and Rayhani 2017)

Aldaeef and Rayhani (2017) stated that "If warm ice-poor permafrost at a temperature of $-1.5^{o}C$ was exposed to warming to a temperature higher than the freezing point, its strength (based on the current experiment) will drop from 0.2MPa to around 0.065MPa showing a reduction of 300% which represents a factor of safety of 3. This means a failure can occur to a structure supported by piles designed with a factor of safety of 3 if a total degradation of the permafrost encountered".

2.10.2 Creep tests by Aldaeef and Rayhani (2017)

Aldaeef and Rayhani (2017) conducted creep tests. The direct shear test apparatus was modified by installing a pulley system so that a constant tangential load could be applied on the steel plate. The modified direct shear test apparatus is shown in Figure 2.6. A similar procedure with adfreeze strength test was repeated to do the creep tests. The sample was frozen with an applied normal stress of 100kPa at the temperature -10^{o}C, and then a 535 kPa tangential load was applied on the steel-soil interface. "When a steady state creep rate observed, the temperature was increased to the next level. This procedure was repeated until pile-soil rupture occurred giving that a steady state creep rate was always attained before increasing the temperature to the warmer level" (Aldaeef and Rayhani 2017).

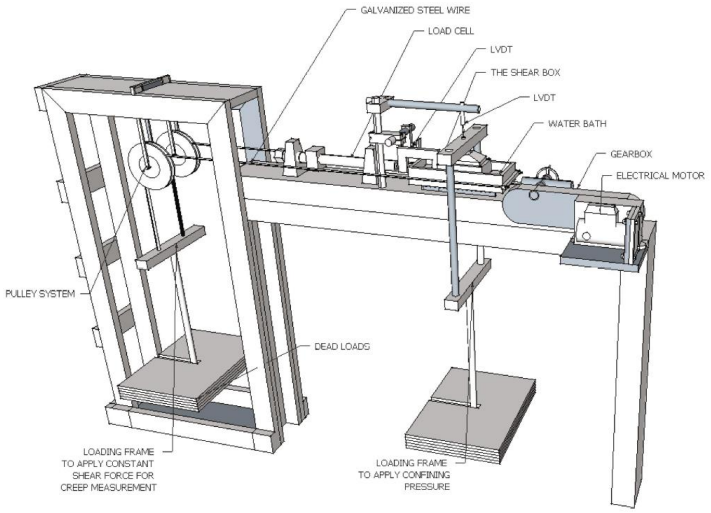

Figure 2.6 Modified direct shear test apparatus (from Aldaeef and Rayhani 2017)

The experimental results are shown in Figure 2.7.

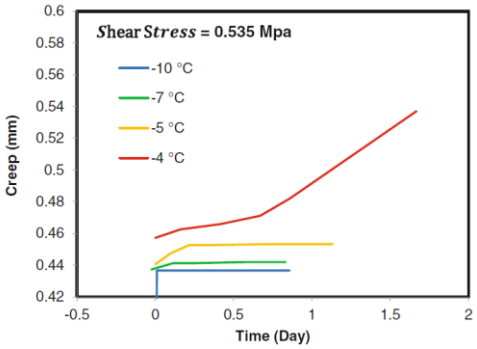

Figure 2.7 The relationship between pile creep behavior and temperature (Aldaeef and Rayhani 2017)

Aldaeef and Rayhani (2017) provided the following observations:

"When the temperature is -10^{o}C, the magnitude of primary creep is 0.44 mm".

"After the primary creep, the secondary creep will begin. The rate of secondary creep is constant and it is equal to 8×10^{-6} mm/h".

"The magnitude of primary creep is 0.0047 mm when increasing the temperature to -7^{o}C from -10^{o}C".

"So the primary creep at -7^{o}C is 1% of the primary creep at -10^{o}C".

"The primary creep at -5^{o}C and -4^{o}C increase 2.7% and 3.1% of the primary creep at -10^{o}C, respectively, with increasing the temperature".

"So due to climate warming, pile foundations in warming permafrost go through primary creep many times when the temperature in permafrost increases". Increasing temperatures have a significant impact on the stability of pile foundations.

The relationship between secondary creep and time is shown in Figure 2.8.

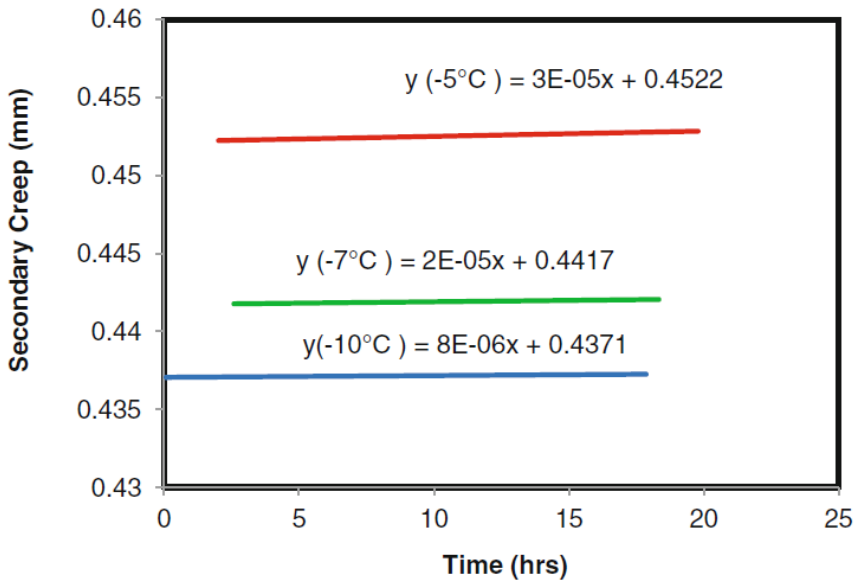

Figure 2.8 The relationship between secondary creep behavior and time (Aldaeef and Rayhani 2017)

Using the experimental data shown in Figure 2.8, Aldaeef and Rayhani (2017) made the following observations:

"The higher the temperature in the permafrost, the faster the secondary creep rate is".

"When increasing the temperature from −10℃ to −5℃, the secondary creep rate increases 60%".

"When the secondary creep increases, the pile foundations will become unstable".

Aldaeef and Rayhani (2017) also analyzed the effects of climate warming on adfreeze strength at the soil-pile interface and creep behavior of pile foundations in permafrost. They stated that "Adfreeze strength includes adhesion strength and friction strength. Temperature increase will cause adfreeze strength decrease and pile creep increase which causes the instability of piles".

2.11 Permafrost Settlement Hazard in Alaska Due To Climate Warming

2.11.1 Introduction

"In Alaska, since 1960s, the temperatures in permafrost have increased which caused thawing of permafrost, thaw settlement of pile foundations and instability of structures built in permafrost" (Hong et al., 2014). Permafrost Settlement Hazard Index (PSHI) was developed by Hong, Perkins and Trainor (2014) to predict the climate warming in permafrost and estimate thaw settlement in Alaska using known climate model by considering the factors that affect thaw subsidence.

"The temperature in permafrost is related to air temperature and ecosystem characteristics such as topography, soil properties, vegetation, snow, surface water" (Smith and Riseborough, 1996; Jorgenson et al., 2010). Increasing temperatures in discontinuous permafrost deserve more attention as the temperature is higher in discontinuous permafrost than that of the temperature in continuous permafrost (Jorgenson et al., 2001; Nelson et al., 2002; ACIA, 2005).

2.11.2 Variables

Hong, Perkins and Trainor (2014) analyzed six ecosystem variables that influence the thaw settlement in Alaska and calculated the PSHI by considering the each variable's risk values. "The six variables are ground ice volume, air temperature, soil texture, snow depth, vegetation and organic content of soil" (Hong et al., 2014).

Ice melting will definitely affect the strength of permafrost (Andersland and Ladanyi, 2004; Smith and Burgess, 2004). Jorgenson et al. (2008) stated that "Ground ice content can be

classified as high, moderate, variable, low or unfrozen". A higher value of PSHI was assigned to ice-rich soils (Hong et al., 2014).

Air temperature is also a factor that will affect the temperature in permafrost (Smith and Burgess, 2004). They reported that the permafrost has a high risk to thaw if the permafrost temperature is higher than -2^{o}C. They also stated that if mean annual air temperature (MAAT) is higher than -2^{o}C, then the permafrost starts to thaw.

"Soil texture is an important factor that will also affect moisture content in the soil and soil thermal properties" (Shur and Jorgenson, 2007; Jorgenson et al., 2010). For example, gravelly soils are easy to drain and fine soils are hard to drain (Hong et al., 2014). Different soils have different ice content according to soil texture (Hong et al., 2014). "Ice-rich soils like fine-grained soils are more likely to undergo thaw settlement" (Andersland and Ladanyi, 2004; Smith and Burgess, 2004).

Snow has low thermal conductivity, therefore heat transfer between air and permafrost is limited (Romanovsky and Osterkamp, 2001; Smith and Burgess, 2004; Camill, 2005; Zhang, 2005). "The impact of snow depth on permafrost relies on the duration, accumulation, and melting processes of snow" (Smith and Burgess, 2004; Zhang, 2005). "So it is difficult to know the effect of snow on frozen soil" (Hong, et al., 2014). Many studies reported that if the snow depth is higher, the temperature of permafrost will be higher (Hong, et al., 2014). Osterkamp et al. (2009) and Jorgenson et al. (2001) show that "snow cover increase caused permafrost degradation in Alaska". Therefore, if snow cover is thicker, the risk number increases (Jorgenson et al., 2001; Osterkamp et al., 2009).

"The vegetation also affects the permafrost temperature by insulating it from the higher atmospheric temperatures" (Jorgenson et al., 2010). According to Shur and Jorgenson (2007), vegetation also makes permafrost resilient to increased air temperature.

The organic layer in the soil also has an important impact on the temperature in permafrost (ACIA, 2005; Jorgenson et al., 2010). "This is because the organic layer in the soil is difficult to drain and has higher thermal conductivity in winter and lower thermal conductivity in summer" (Hong et al., 2014). The organic layer in the soil can, therefore, contribute to heat loss in winter while reducing heat exchanges during the summer, and thus maintaining a colder temperature (Romanovsky and Osterkamp, 1995). As a result, a lower risk value can be assigned to organic soils (Hong et al., 2014).

2.11.3 Results

Figure 2.9 shows the permafrost settlement hazard index map for the U.S. state of Alaska.

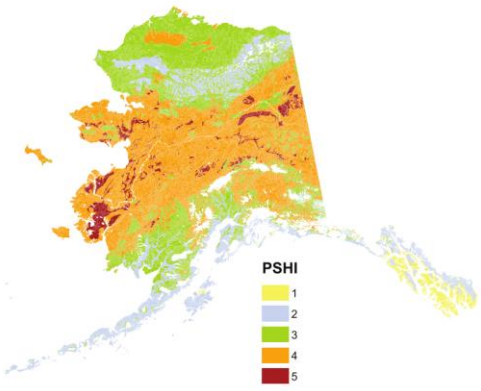

Figure 2.9 Permafrost Settlement Hazard Index map (Hong et al., 2014)

"The PSHI was developed to enable analysis of anticipated thaw subsidence caused by climate warming. The colors on the map represent rounded numerical PSHI values from 1 (lowest) to 5 (highest). The higher the value is, the greater the risk of thaw subsidence of the permafrost" (Hong et al., 2014).

CHAPTER THREE

ASSESSMENT OF CONFINING PRESSURE ACTING ON PILE SHAFT AS A RESULT OF COMPACTION AND TEMPERATURE CHANGES

The solar panels installed in the region of Cornwall, Ontario are supported by piles. One of the considerations in the design of these piles is their behavior at various temperatures including the temperatures below freezing. Before freezing of soil water takes place, a reduction in ground temperature results in shrinkage in the soil mass. Once the temperature drops below zero degrees Celsius, soil water starts freezing. Ice forms in the voids of the soil. While the ice is forming and tends to cause expansion of the soil mass, the soil skeleton itself tends to continue to shrink as the temperature drops further. The total volume change of the soil mass ultimately depends on the relative magnitudes of the expansion due to ice formation and the shrinkage of the soil skeleton. These two opposing processes have an effect on the confining pressure acting on the pile shaft. In addition, when the soil water freezes on the pile shaft, it generates bond (adhesion) between the pile shaft and the soil. For the design of these piles, it is necessary to determine the adfreeze bond strength of the interface between the soil and the piles. In the present study, an experiment is carried out to determine the confining pressure (lateral normal stress) acting on a pile shaft upon freezing. This will allow us to know the magnitude of the normal stress to be applied in adfreeze bond strength tests using the modified direct shear type interface apparatus. In this chapter, the data obtained from cold room experiments are presented. In addition, the scale effect of containers on the magnitude of confining pressure is explored. Adfreeze tests using the modified interface apparatus are described in Chapter 4.

3.1 Soil Characterisation

3.1.1 Sieve Analysis

A sieve analysis was conducted according to ASTM D 2487-98 to classify the Cornwall sand. Table 3.1 is the numerical data of the sieve analysis and Figure 3.1 is the graphical representation.

Table 3.1 Grain size distribution of Cornwall sand

Size(mm)	Sieve#	Sieve weight (g)	Sieve and sample (g)	Mass retained (g)	Cummulative (g)	Passing %
4.75	4	516.35	516.35	0	0	100
1.7	12	439.77	502.77	63	63	79.7
0.6	30	410.69	498.79	88.1	151.1	51.4
0.425	40	387.22	412.60	25.38	176.48	43
0.25	60	365.94	406.39	40.45	216.93	30.2
0.18	80	362.81	384.41	21.6	238.53	23.3
0.15	100	351.52	362.69	11.17	249.7	19.7
0.075	200	344.11	375.44	31.33	281.03	9.6

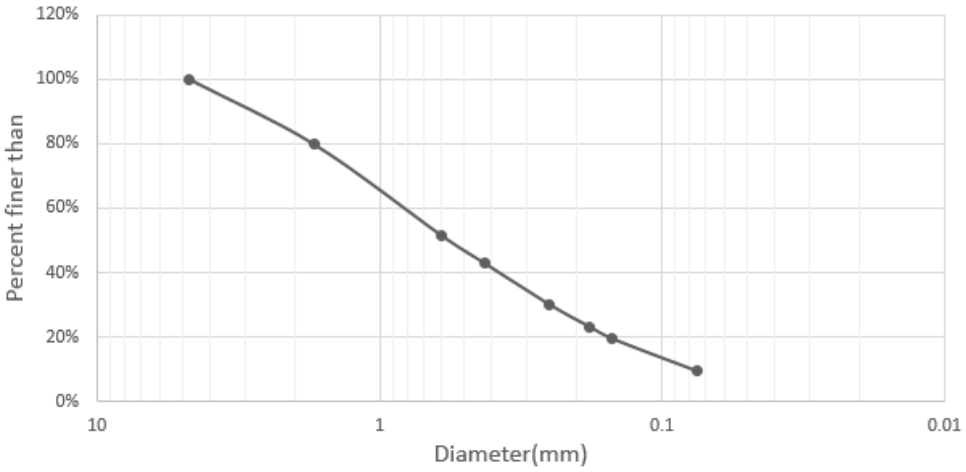

Figure 3.1 Grain size distribution of Cornwall sand

The coefficient of uniformity C_u and the coefficient of curvature C_c are defined below:

D_{10}= 0.075mm D_{30}= 0.25mm D_{60}= 0.83mm

$$C_u = \frac{D_{60}}{D_{10}} = \frac{0.83\text{mm}}{0.075\text{mm}} = 11.06 \qquad \text{Eq. 3.1}$$

$$C_c = \frac{(D_{30})^2}{D_{10} * D_{60}} = \frac{0.25^2}{0.075 * 0.83} = 1 \qquad \text{Eq. 3.2}$$

According to Unified Soil Classification System (USCS), $C_u \geq 6$ and $1 \leq C_c \leq 3$, Cornwall sand can be classified as a well-graded sand.

3.1.2 Standard Proctor Test

To get the relationship between dry density of soil and water content, standard Proctor test was conducted according to ASTM Standard D698 by Villeneuve (2017).

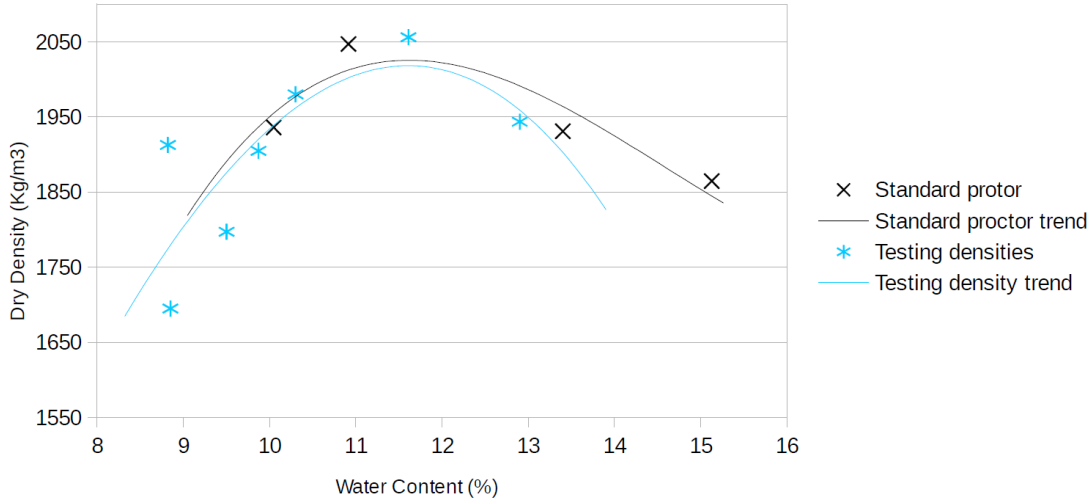

Figure 3.2 Standard Proctor curve and test densities in pull-out tests (From Villeneuve, 2017)

3.2 Experimental set-up

In the experiments to determine the confining pressure acting on a pile shaft, a modified freezer (also referred as "cold room") in the structural lab at the University of Ottawa was used. The experimental setup includes a PVC container, a PVC tube representing the pile, strain gages, a strain indicator, thermistors, Raspberry PI used as a data logger, a monitor, and a freezer. A picture of the test setup is given in Figure 3.3. The two pictures at the top of the figure are the view of the same container from different directions. Strain indicators are used to take readings of the strain gage. The Raspberry PI was used to take readings of the thermistors and monitor the temperature of the soil. A plastic sheet was used to cover the top of the container to prevent moisture loss during experiments. The steps during the preparation and running the experiments are described below.

First, a strain gage is attached on the inside surface near the bottom of the PVC tube. This strain gage is used to measure the hoop strain in the tube. Hoop strain increases with increasing confining pressure. The method used to relate the hoop strain and confining pressure is described at the end of this chapter. A thermistor was put in the soil at the same level with the strain gage to monitor the temperature of the soil.

The height of the tube is 270mm. The outside diameter of the tube is 106mm and the wall thickness is 3mm. A wire was soldered to the strain gage. The wire was then connected to the strain indicator which was used to take readings of the strain gage. Subsequently, the container (see Figure 3.3) was put in the cold room without starting the freezer. At that point, the cold room was at the room temperature (20^{o}C). The tube was placed in the center of the container which has a height of 300mm and a diameter of 300mm. While the temperature in the cold room was still at room temperature, the container was filled with sand which had 11%

gravimetric water content. The soil in the container was compacted layer by layer until the desired thickness was reached to get the maximum dry density. The reason for compacting soil to its maximum dry density is because Villeneuve used maximum dry density in his pull-out tests. After the compaction, the sand level was 1 cm below the top of the tube. Strain gage readings were taken at the beginning and at the end of compaction of soil. The confining pressure generated by compaction is calculated from the strain measured at that stage of the experiment. Once the preparation of the sample was completed, the cold room was activated.

Figure 3.3 Experimental set up for the measurement of confining pressure (The height of the tube is 270mm. The outside diameter of the tube is 106mm and the wall thickness is 3mm.

The container has a height of 300mm and a diameter of 300mm. The container thickness is 9mm.)

Soil temperatures and strain readings were recorded as temperature in the freezer decreased. The relationship between soil temperature and strain readings are presented in Figure 3.4 for the larger diameter tube case and Figure 3.5 for the smaller diameter tube case.

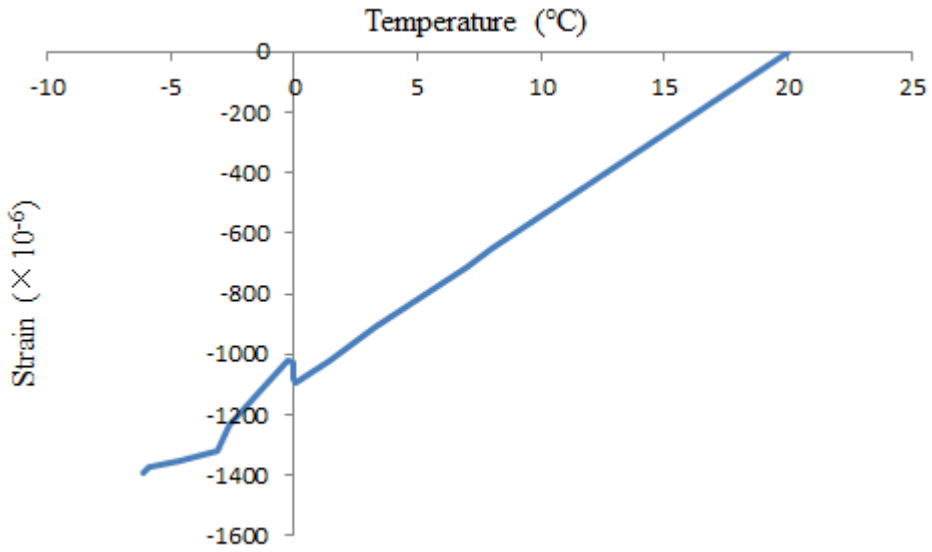

Figure 3.4 Hoop strain variations with temperature in the larger diameter tube (inside diameter=100mm) embedded in soil. Water content is 11%. The effect of compaction is not included in this figure. The negative sign on the vertical axis indicates that the hoop strain is compressive.

The chemical composition of the sand was not determined experimentally. However, in the cold room experiments, the bump shown below 0^{o}C in Figure 3.4 and Figure 3.5 indicates that the soil water started to freeze at 0^{o}C. That means there is not sufficient amount of salt in the water to affect its freezing temperature.

Confining pressure acting on tube shaft includes two components, one is the confining pressure due to compaction and soil weight, and the other is the confining pressure due to

temperature changes during freezing. For the larger diameter tube embedded in soil, the strain caused by compaction and soil weight is 196 $\times 10^{-6}$, which means that the confining pressure due to compaction and soil weight is 69.04kPa by using the calibration results in section 3.3.

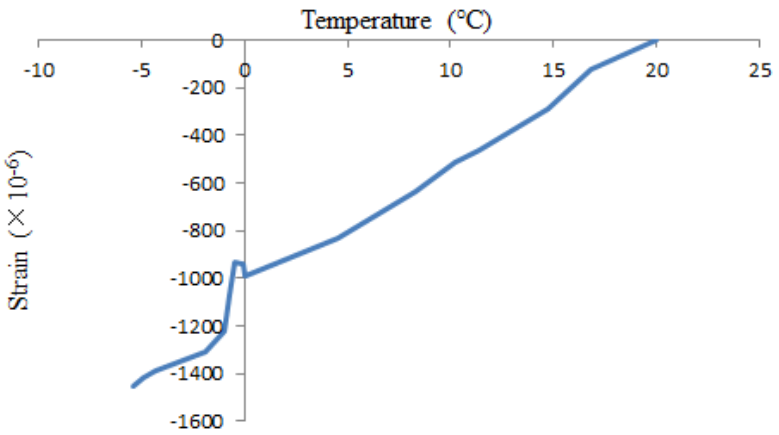

Figure 3.5 Hoop strain variations with temperature in the smaller diameter tube

For the smaller tube embedded in soil, the strain caused by compaction and soil weight is 338 $\times 10^{-6}$, which means the confining pressure due to compaction and soil weight is 119.07kPa by using the calibration results in section 3.3.

3.3 Strain gage calibration

The readings of the strain gage were calibrated through the use of a sphygmomanometer (blood pressure monitor) depicted in Figure 3.6. The calibration is used to convert the hoop strains measured by the strain gage fixed inside the tube to confining pressure causing it. For this purpose, the sphygmomanometer was used to apply a known external pressure on the tube used in the experiments. The relationship between strain variation and readings of the

sphygmomanometer is shown in Figure 3.7. The dial gage of the sphygmomanometer provides the readings in mmHg which can be directly converted to kPa (1 mmHg=0.1333 kPa). The relationship between strain variation and confining pressure in kPa is shown in Figure 3.8.

Figure 3.6 Blood pressure monitor

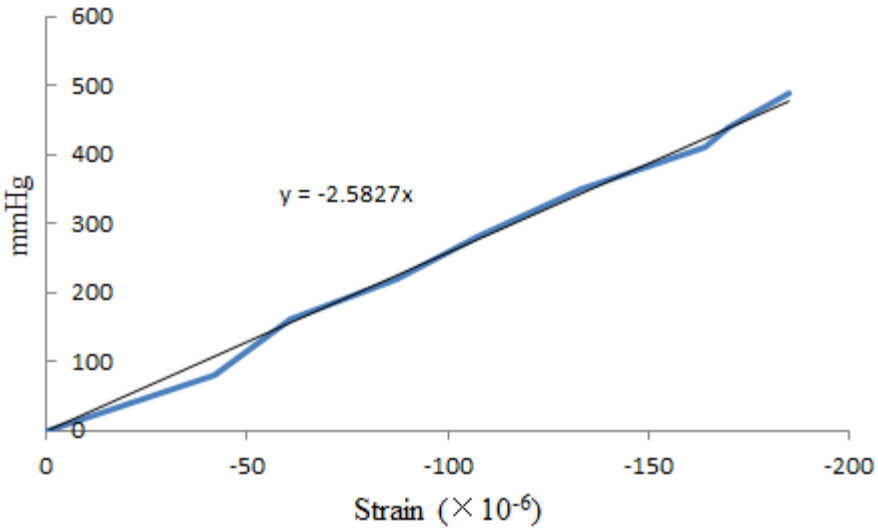

Figure 3.7 Relationship between strain variation and readings of the sphygmomanometer

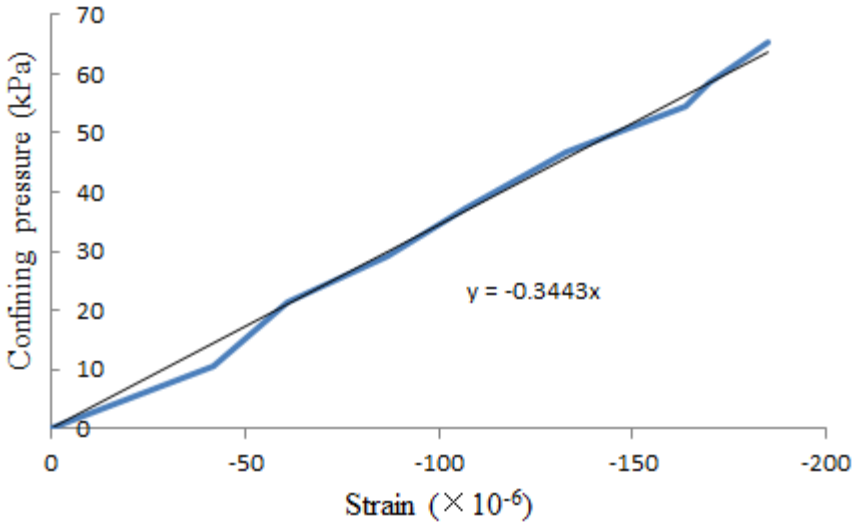

Figure 3.8 Relationship between strain variation and confining pressure acting on the 100mm diameter tube

3.4 Experimental results relating the confining pressure to compaction and temperature change

Using the equation provided in Figure 3.8, the hoop strains shown in Figures 3.4 and 3.5 are converted to confining pressures. The results are shown in Figures 3.9 and 3.11. Note that, the effect of compaction and soil weight is not added to the effect of temperature change in these two figures.

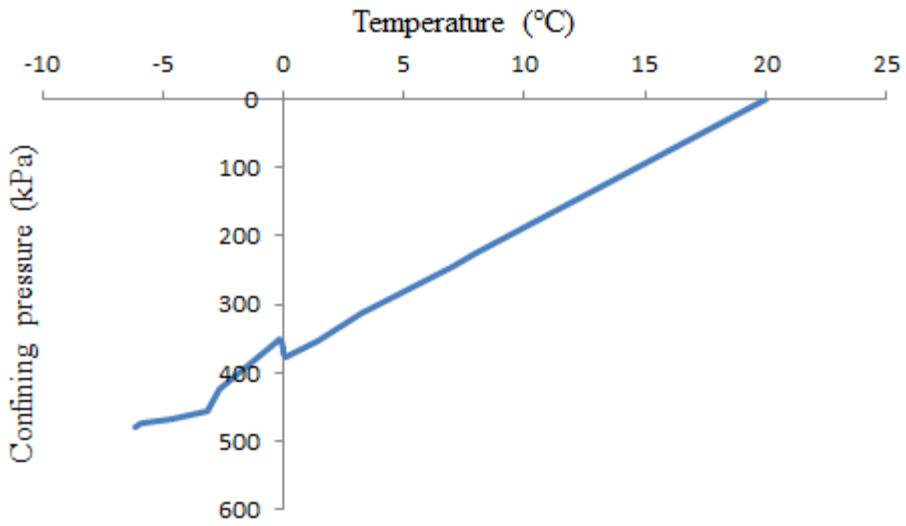

Figure 3.9 Confining pressure acting on pile shaft due to freezing (larger diameter tube embedded in soil)

According to Figure 3.9, the confining pressure acting on the tube shaft increases when the temperature decreases from 20°C to 0°C as the soil skeleton would shrink in the direction of the tube. It should be noted that there is a bump in Figure 3.9 below 0°C, this is because the unfrozen water in the soil starts to freeze and the soil skeleton would expand in the direction of the container, so the hoop strain in the tube will decrease. After the bump, the confining pressure starts to increase again because the soil skeleton and ice volume would shrink.

According to Figure 3.9, at -5°C, the confining pressure acting on larger diameter tube shaft due to freezing is 468.69kPa, this value looks large and it has to be verified by another test in the future.

For the larger tube embedded in soil, the confining pressure acting on tube shaft due to compaction and soil weight is 69.04kPa. The effect of compaction and soil weight on the confining pressure should be added to the confining pressure resulting from temperature

change. Therefore, the confining pressure acting on larger diameter tube shaft is 537.73kPa at -5℃ as shown in Figure 3.10.

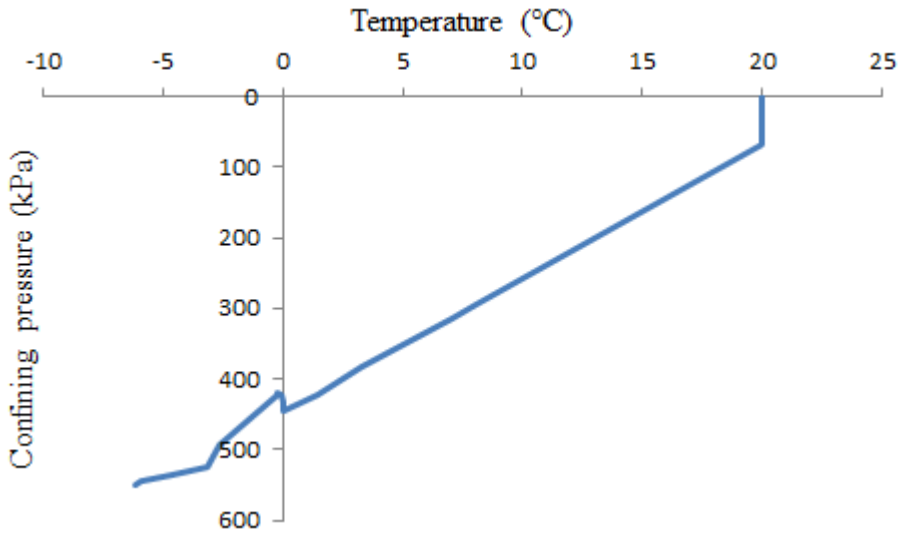

Figure 3. 10 Confining pressure acting on tube shaft (larger diameter tube embedded in soil)

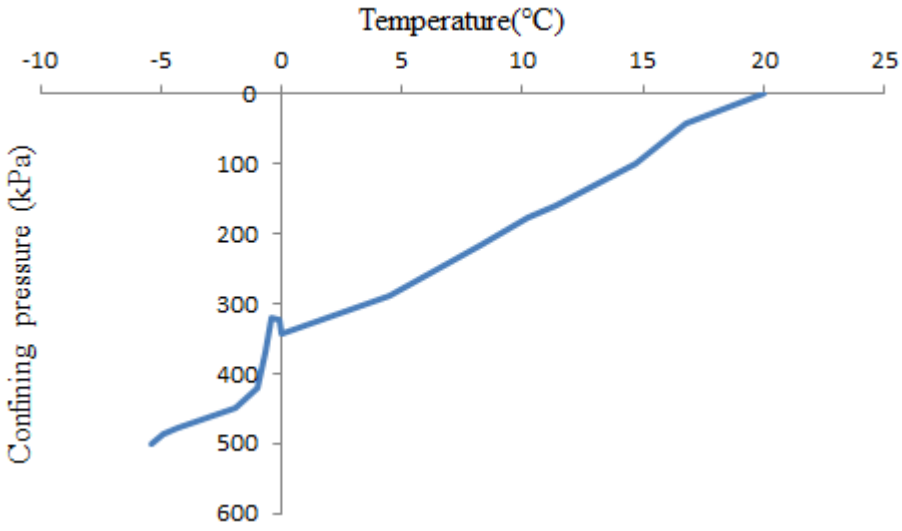

Figure 3.11 Confining pressure acting on tube shaft due to freezing (smaller diameter tube embedded in soil)

According to Figure 3.11, the confining pressure acting on the smaller diameter tube shaft due to freezing is 489.56kPa at -5°C temperature, this value looks large and it has to be verified by another test in the future.

For the smaller diameter tube embedded in soil, the confining pressure acting on tube shaft due to compaction and soil weight is 119.07kPa.The effect of compaction and soil weight on the confining pressure should be added to the confining pressure resulting from temperature change. Therefore, the confining pressure acting on smaller diameter tube shaft is 608.63kPa at -5°C as shown in Figure 3.12.

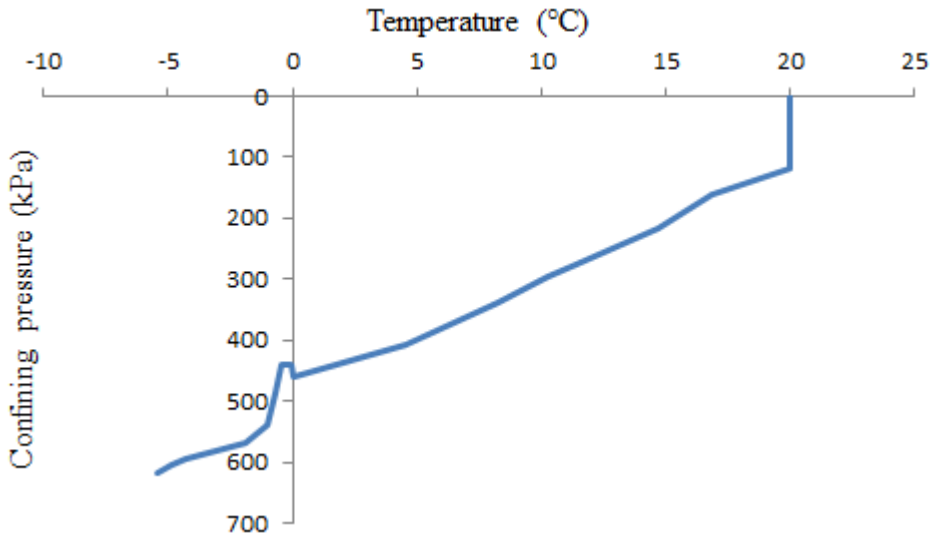

Figure 3.12 Confining pressure acting on tube shaft (smaller diameter tube embedded in soil)

In real life, the soil around a pile is not compacted. In the present study, it was necessary to compact the soil so that the experimental data presented above can be used to interpret the data from Villeneuve's pull-out tests. Villeneuve (2017) also compacted the soil the same way it is done in the present work.

CHAPTER FOUR

EXPERIMENTS FOR THE DETERMINATION OF ADFREEZE BOND STRENGTH OF SOIL-STEEL PLATE INTERFACES

The objective of following experimental study is to determine the adfreeze bond strength of an interface between Cornwall Sand and a steel plate. The model scale pile used by Villeneuve (2017) in his pull-out tests is made of steel. In addition, steel plates were used by Villeneuve (2017) in his interface tests in the geotechnical graduate laboratory. It is therefore assumed that the results obtained in the present work can be used in the analysis of pull-out tests of Villeneuve (2017).

It was difficult to insulate the interface apparatus (C3DSSI) for its use in freezing temperatures (Villeneuve, 2017). In the present study, it was decided to use a different apparatus. In order to measure the adfreeze bond strength of the interface in freezing temperatures, a conventional direct shear apparatus is modified.

4.1 Modified Direct Shear Apparatus

In the design of piles in cold regions, axially applied loads are assumed to be carried only by adfreeze bond and the contribution of the end bearing capacity is generally neglected. The reason for this engineering practice is related to the large displacement required in order to fully mobilize the toe capacity. The settlement required for the end bearing capacity (toe resistance) to reach its full value is a lot more than the displacement required for the shaft resistance to develop (Andersland and Ladanyi, 2004).

For testing interfaces in the present study, a fully automated direct shear test apparatus available in the laboratory was used. Displacement rate is controlled by an electronic controller built into the apparatus. Load cells and displacement transducers are connected to an external computer and data acquisition system.

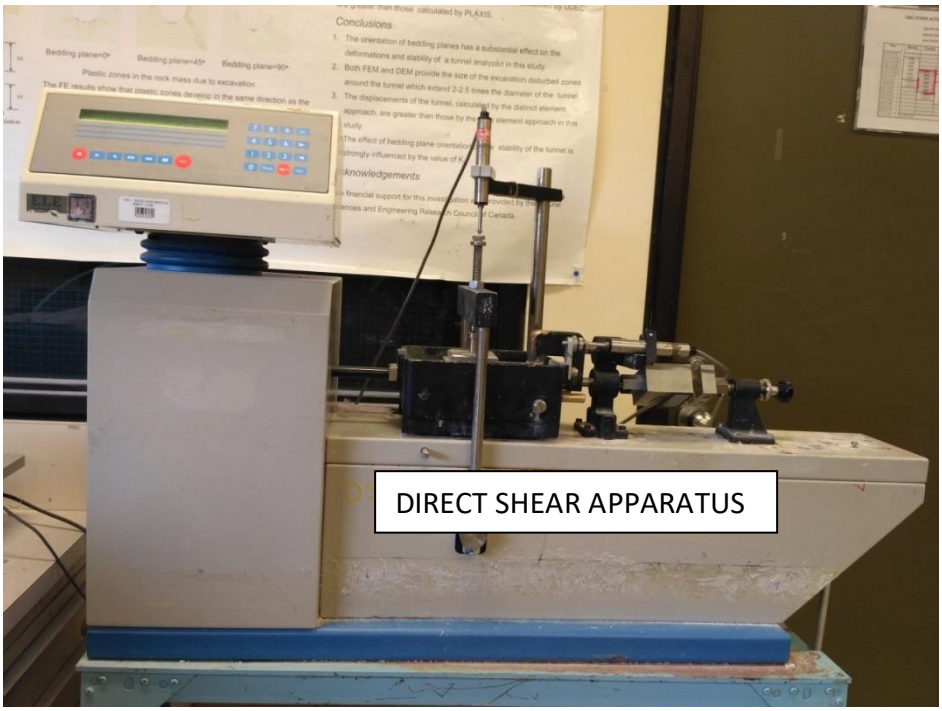

Figure 4.1 Conventional direct shear apparatus Modifications have been made in this apparatus as described below.

The conventional direct shear apparatus located in the geotechnical lab of the University of Ottawa is shown in Figure 4.1. When unmodified, this apparatus can be used to measure the shear strength of the soils at room temperatures. For determining the shear strength of the interface between the soil and the steel plate at freezing temperatures, two modifications were necessary: (1) Replace the soil in the lower half of the soil container with a steel plate to allow for interface testing, and (2) provide an insulated enclosure within encompassing the specimen cell. This enclosure will be referred to as the “test chamber” for the remainder

of this chapter. The temperature within the test chamber can be lowered to -5^{o}C through the use of two vortex tubes. The vortex tubes injected cold air into the chamber. Most of the experiments were conducted at -5^{o}C with an accuracy of ±1^{o}C.

A picture of the modified apparatus is shown in Figure 4.2. The soil sample and shear box were held by bolted plates in the experiment. A motor was used to advance the lower part of the shear box in the horizontal direction. The soil sample in the upper part of the shear box was kept stationary. One strain gage displacement sensor (SGD) was used to measure the horizontal displacements. Vertical displacements were measures by another SGD shown in the figure.

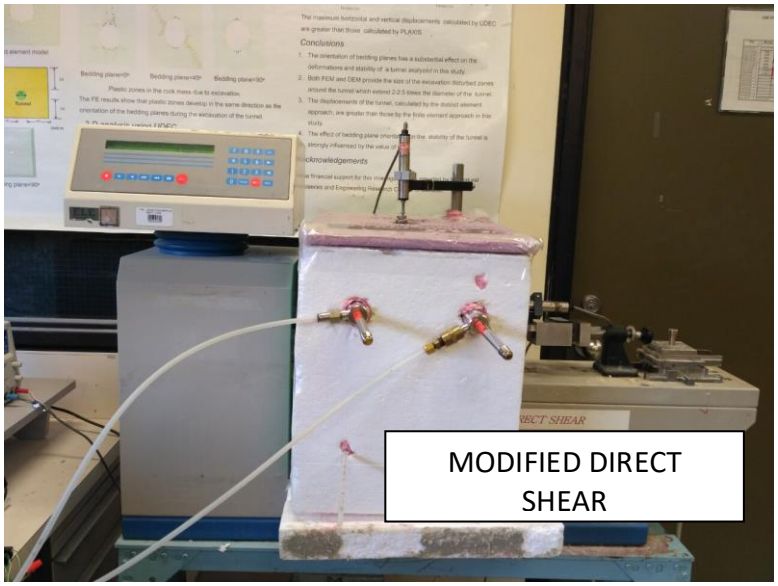

(a)

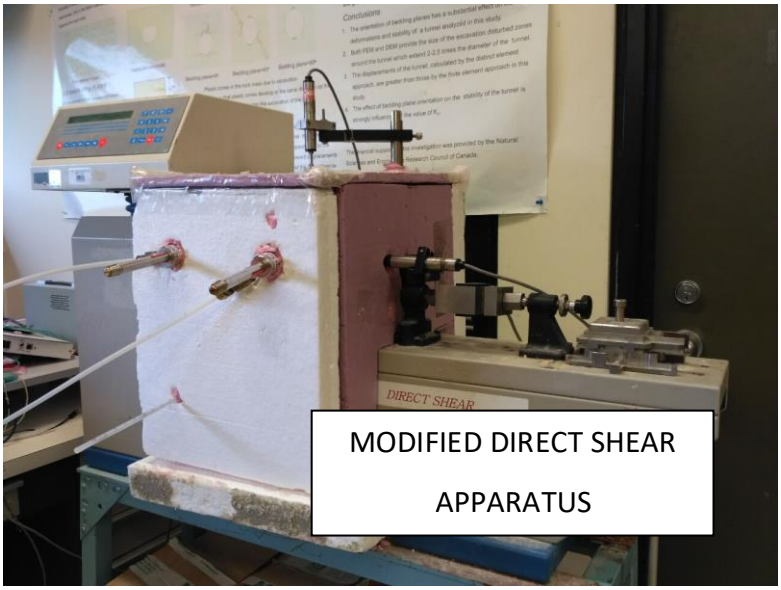

(b)

Figure 4.2 Pictures of the modified direct shear apparatus with thermal insulations (a) Front view showing the insulation and two vortex tubes, (b) Side view showing the insulation at the top and on the side.

4.2 Sample Preparation

The soil used in the experiment was Cornwall Sand from Ontario in Canada. Soil particles bigger than 1.7mm were removed in the sample preparation process. Figure 4.3 shows the assembled parts of the shear box. The figure also shows at the very top a loading plate attached to a bolt to apply vertical load on the soil sample. Figure 4.4 is the lower shear box which contains the steel plate of the interface. Figure 4.5 shows the upper shear box with soil. The dimensions of the upper shear box are 60mm×60mm×21mm (length, width, height). The dimensions of the lower shear box are 60mm×60mm×25mm (length, width, height). The gravimetric water contents of the soil samples are 9%, 11% and 13%. At 9%, 11% and 13% water contents, the dry densities of the soil samples are 2062.16 kg/m^3, 2025 kg/m^3 and 1989.16 kg/m^3, respectively. Three soil samples are prepared for each water content. Three soil samples prepared for each soil water content were subjected to normal stresses of 25kPa, 45kPa and 80kPa.

Vortex tubes were used for 14 hours for the soil samples to freeze completely and to develop adfreeze bond between the soil sample and the steel plate. A thermometer was used to monitor the air temperature of the testing chamber. Horizontal displacements were applied by the motor of the apparatus in the horizontal direction after the adfreeze bond was formed.

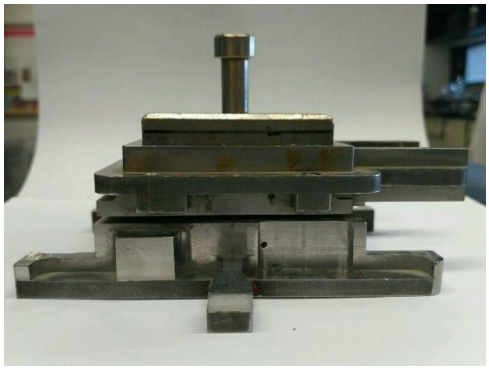

Figure 4.3 Assembled interface shear box: upper and lower parts of the shear box and the loading plate to apply vertical load on the soil-steel plate interface

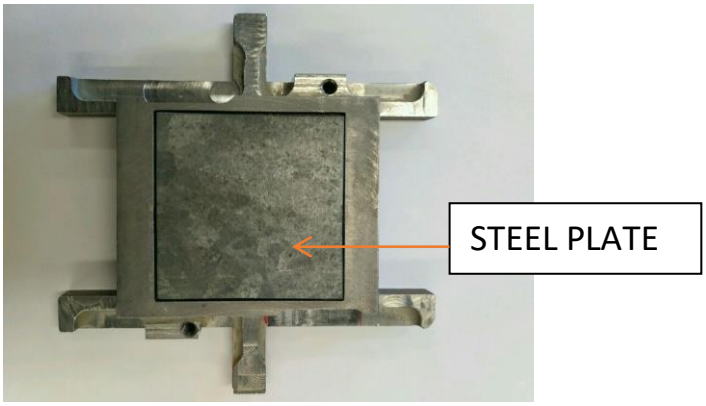

Figure 4.4 Lower part of the shear box, a view from the top

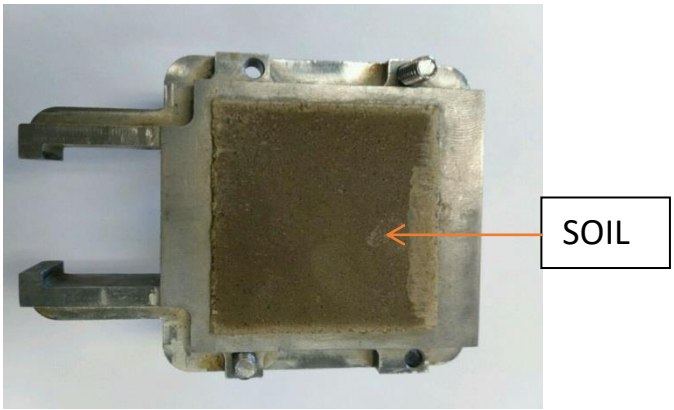

Figure 4.5 Upper part of the shear box with soil, a view from the top

4.3 Pile Material

In the soil-steel plate interface testing experiments, the pile material used was corrugated galvanized sheeting. A Hommel Tester T500 roughness meter was used to measure the roughness of the corrugated galvanized sheeting by Villeneuve (2017). The roughness measurement device can read the average roughness R_a, the range of roughness R_r and maximum roughness R_m. The precision is 0.1 μm. The measurement process was done at different locations and directions on the surface of the sheeting. The roughness measurement results can be found in Table 4.1.

Table 4.1 Sheeting roughness measurement results (Villeneuve, 2017)

R_z (μm)	23.76	17.78	16.76	18.60
R_a (μm)	3.74	2.50	2.66	2.50
R_T (μm)	31.22	23.30	18.90	28.00

4.4 Apparatus Settings

In the adfreeze experiments, the motor was set to move in the horizontal direction at a rate of 0.1mm/min. The system is composed of a computer, a controller, a load cell for measuring the horizontal load applied to the interface, two SGDs to measure the horizontal and vertical displacements, and the modified interface testing apparatus.

4.5 Experimental results

In the following, the horizontal displacements versus shear stress curves from all interface tests are shown. There are three groups of tests related to different moisture contents. There are also three different tests in each group. The interfaces in the same group are subjected to

normal loads resulting in 25kPa, 45kPa, and 80 kPa normal stresses. According to Weaver and Morgenstern (1981), the normal stress acting on a pile shaft is smaller than 100 kPa in the field applications. In the present study, the magnitudes of normal stress used in interface tests are chosen 25kPa, 45kPa and 80kPa.

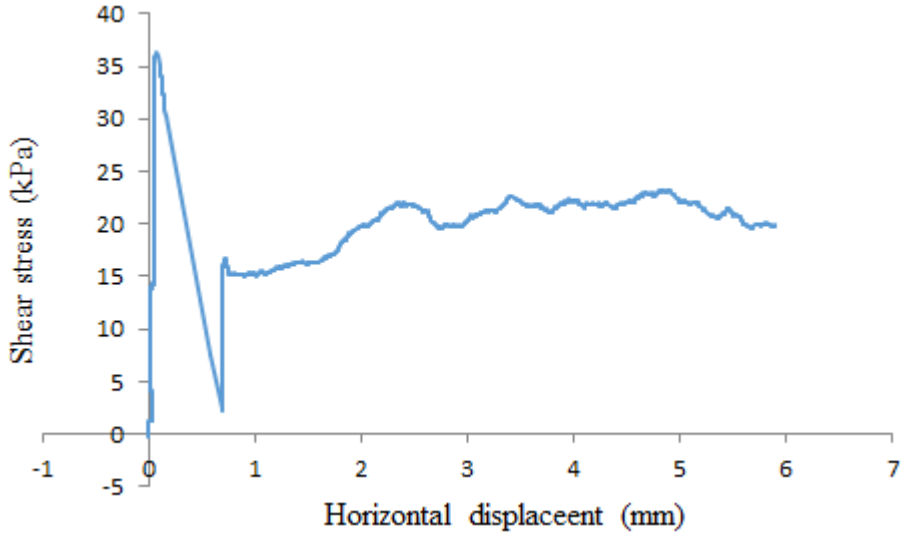

Figure 4.6 Stress-displacement curve for 25kPa normal stress at 9% water content

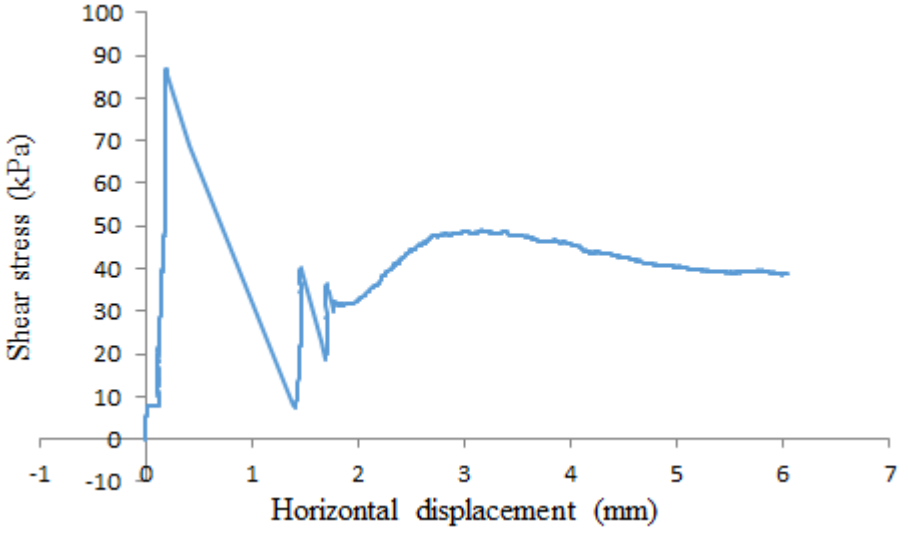

Figure 4.7 Stress-displacement curve for 45kPa normal stress at 9% water content

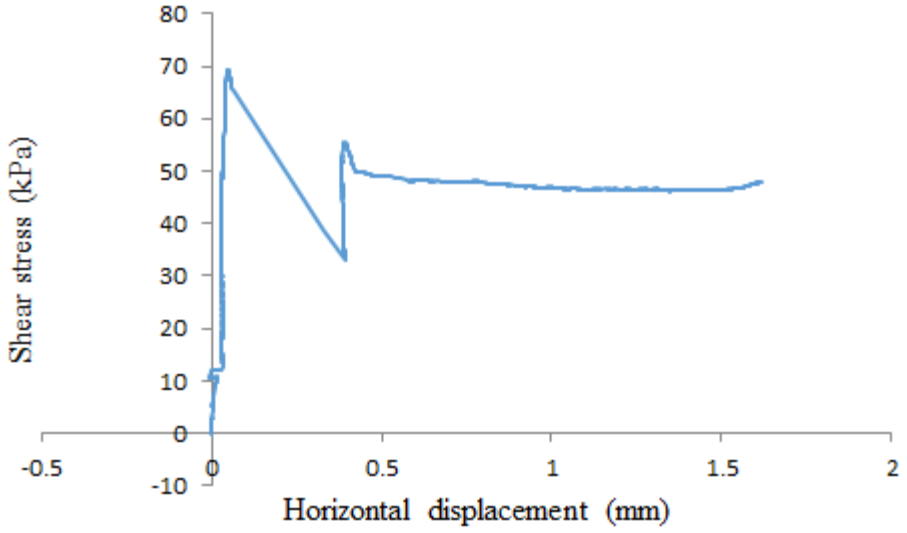

Figure 4.8 Stress-displacement curve for 80kPa normal stress at 9% water content

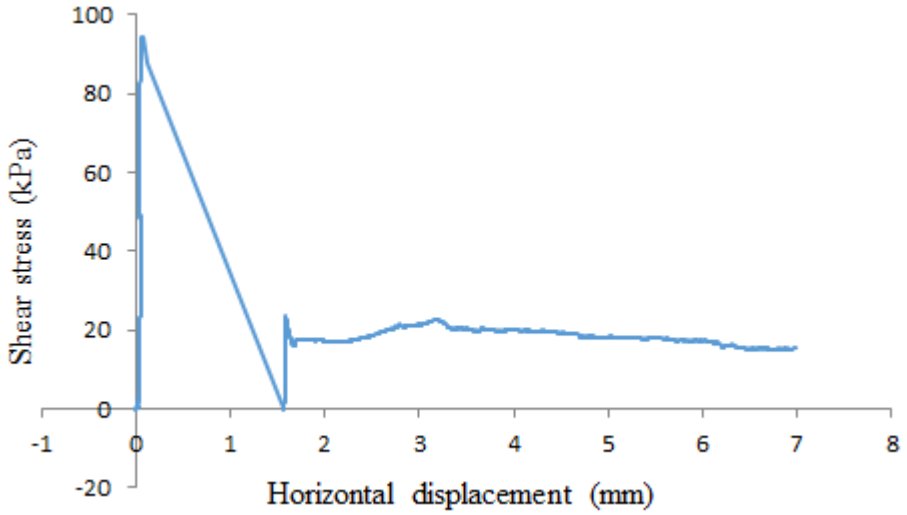

Figure 4.9 Stress-displacement curve for 25kPa normal stress at 11% water content

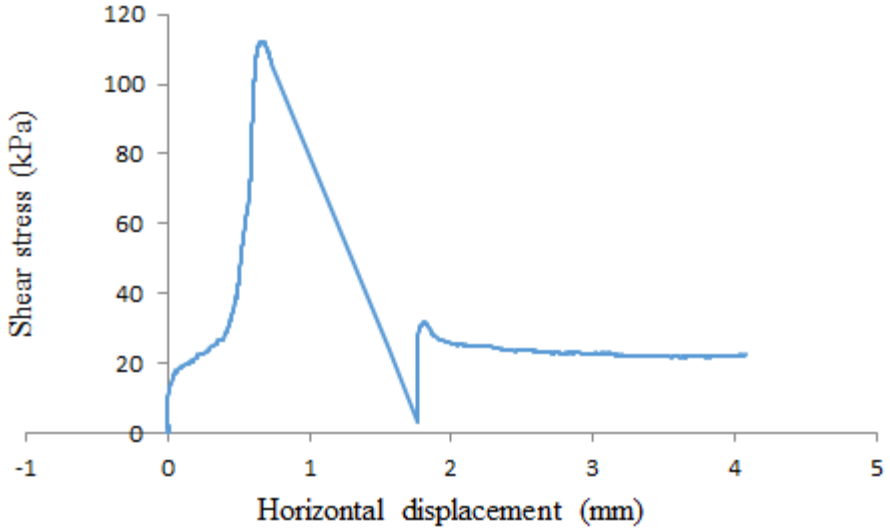

Figure 4.10 Stress-displacement curve for 45kPa normal stress at 11% water content

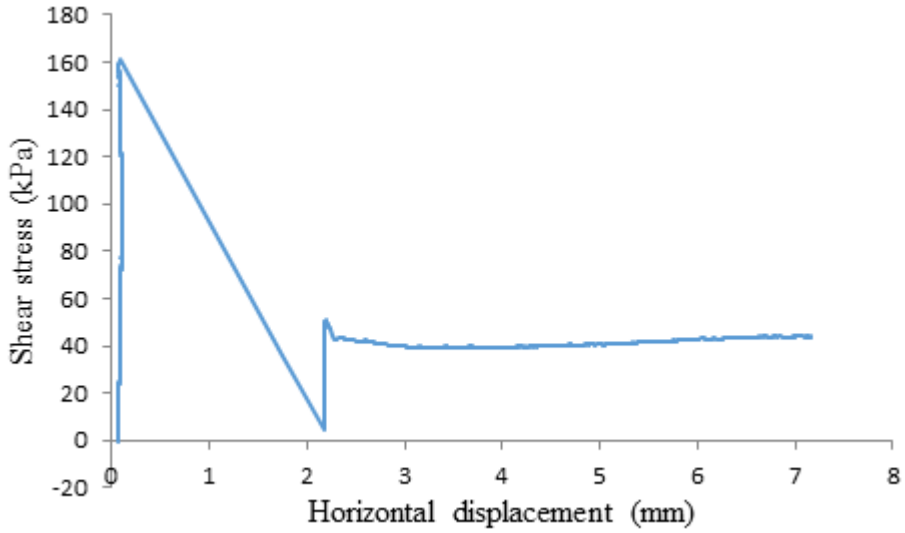

Figure 4.11 Stress-displacement curve for 80kPa normal stress at 11% water content

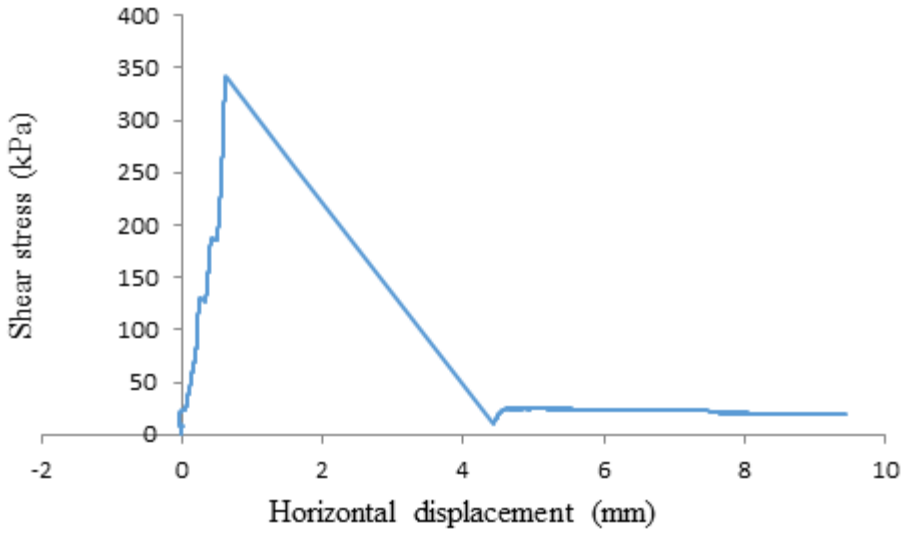

Figure 4.12 Stress-displacement curve for 25kPa normal stress at 13% water content

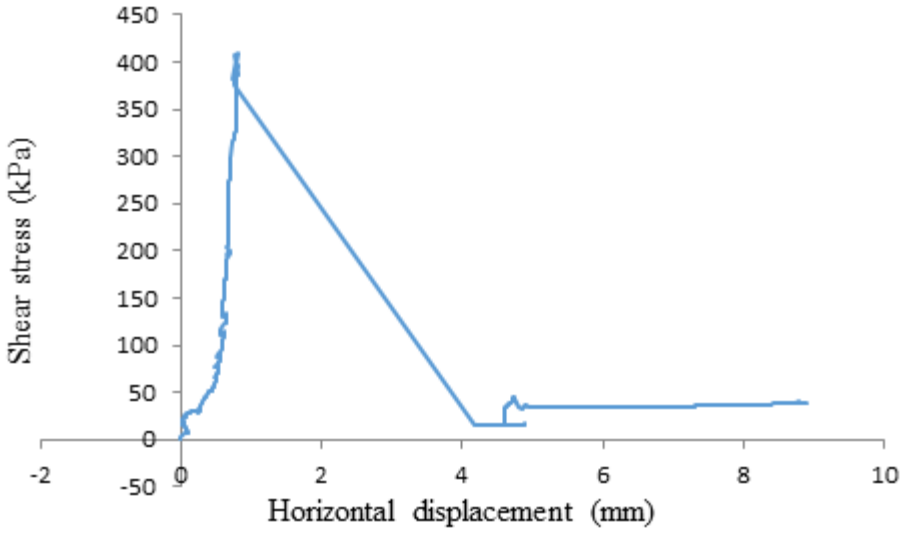

Figure 4.13 Stress-displacement curve for 45kPa normal stress at 13% water content

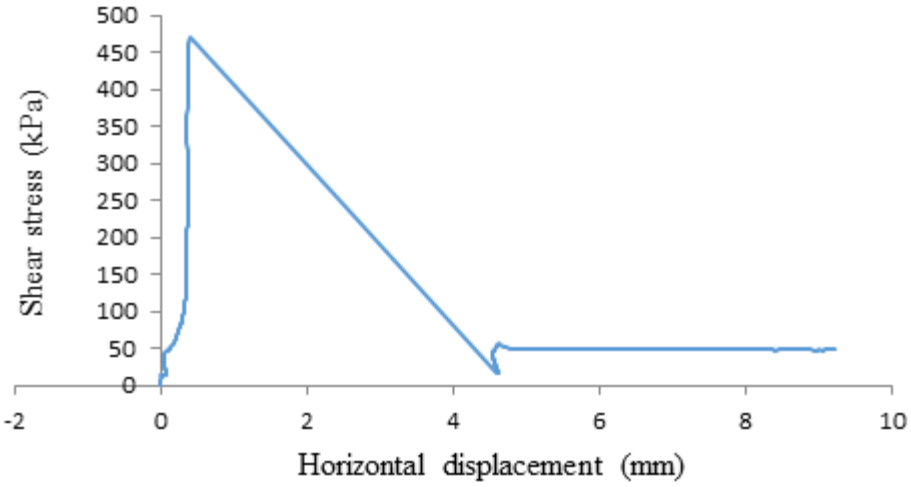

Figure 4.14 Stress-displacement curve for 80kPa normal stress at 13% water content

Figure 4.6 to Figure 4.14 are the pile-soil interface test results at three water contents including 9%, 11%, 13% water content. For each water content value, a normal stress was applied separately on a separate sample. The magnitudes of normal stresses used in the experiments were 25kPa, 45kPa and 80kPa.

Table 4.2 The results of soil-steel plate interface tests

Test	Peak strength, kPa	Residual strength, kPa
9%, σ_n = 25kPa	36	20
9%, σ_n = 45kPa	86	40
9%, σ_n = 80kPa	70	48
11%, σ_n = 25kPa	94	20
11%, σ_n = 45kPa	112	40
11%, σ_n = 80Kpa	160	69
13%, σ_n = 25kPa	341	20
13%, σ_n = 45kPa	409	37
13%, σ_n = 80kPa	470	49

σ_n = Normal stress acting on the interface

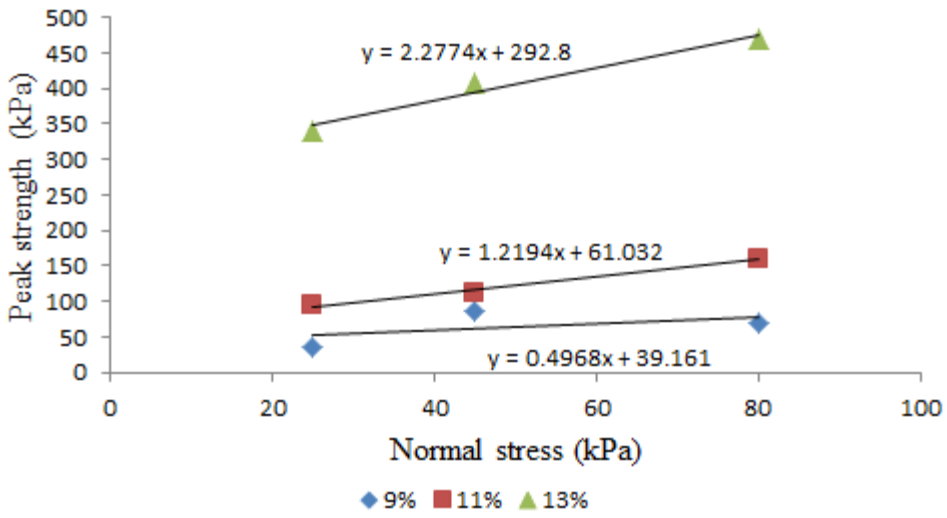

Figure 4.15 Relationship between water content, normal stress and peak strength

Figure 4.15 shows that the peak strength (adfreeze strength) increases with increasing normal stress for the samples tested at the same water content. For the samples with higher water contents, higher adfreeze strengths are observed.

The rupture of the adfreeze bond in all interface tests occurred at a horizontal displacement ranged from 0.1 to 1 mm. “Due to freezing, the interface strength showed a brittle failure mode where a significant strength loss recorded right beyond the peak. This failure mode might be attributed to the viscoelastic behavior of frozen soils” (Aldaeef and Rayhani, 2017).

CHAPTER FIVE

NUMERICAL MODELLING

This chapter describes the numerical analysis carried out using the finite element software PLAXIS to investigate the response of soil samples in cold room experiments to temperature changes ranging from room temperature 20^{o}C to -5^{o}C. These calculations are related to the model scale physical experiments conducted in the cold room that are described in Chapter 3. Those experiments showed that temperature changes have a significant effect on the sample deformations and the stresses acting on the model scale pile.

Similar to the model scale tests, the effect of changing temperatures on the deformations of a cylindrical soil sample is investigated using a simple finite element analysis. This is an axisymmetric problem. The analysis can be classified as a coupled Thermo-Mechanical (TM) type. The effect of water flow is not included in the analysis. The following figure shows the geometry of the soil sample analyzed. The temperatures of the boundaries of the analysis domain were specified as a function of time. The mechanical boundary conditions are shown in Figure 5.1. The soil sample was subjected to, first, decreasing and then increasing temperatures both in the analysis and in the cold room.

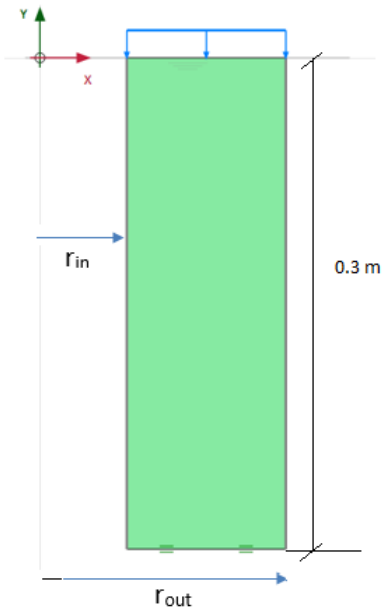

Figure 5.1 Geometry of the axisymmetric domain analyzed by PLAXIS FE code

In this preliminary analysis, only the soil body is considered. The pile and the container are not included in the calculations. The height of soil sample is 0.3 m. The inner radius (r_{in}) is 0.05 m and the outer radius (r_{out}) is 0.15 m.

The parameters used in the following analyses were taken from the PLAXIS tutorials.

5.1 Analysis type 1

Temperatures in the boundaries of the soil domain are decreased gradually from 20^{o}C to -5^{o}C. The possibility of moisture movement in the soil is overlooked. The coefficient of thermal expansion (α) used in the analysis was 5.2e^{-6} (1/K) for the temperatures above zero Celsius. It is assumed that the soil water freezes at zero Celsius and its volume increases by about 9%. The expansion of water turning into ice is simulated by using a negative value for the coefficient of thermal expansion (-5.2e^{-5} unit of 1/K). This value of (α) is a function of

the degree of saturation of the soil sample. The elastic modulus and the Poisson's ratio used in this analysis were $43e^3$ kN/m^2 and 0.3, respectively.

Stages of analysis:

Stage 1: Temperature is reduced from room temperature (20°C) to 0°C.

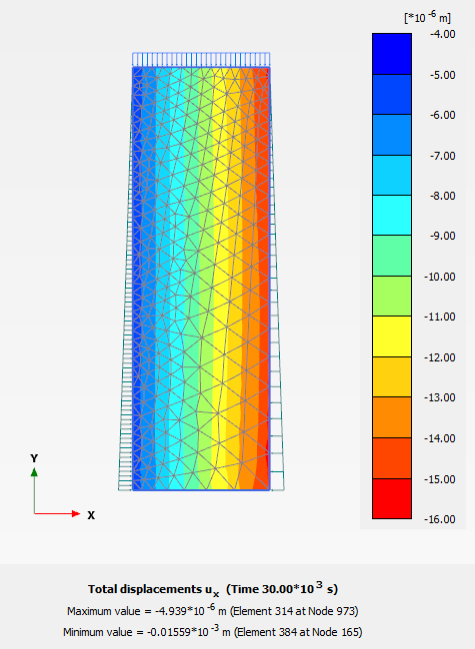

Figure 5.2 Horizontal displacement of the soil sample when the temperature is reduced from room temperature to 0°C

The vertical color code shows that both r_{in} and r_{out} decreased steadily as the temperature was reduced gradually from room temperature down to 0°C. While the reduction in r_{in} was -$4.94e^{-6}$ meters and the reduction in r_{out} was about -$16e^{-6}$ meters. In this stage, the soil sample shrinks and both the inner and outer vertical boundaries move to the left.

Stage 2: Temperature is reduced from 0°C to -1°C.

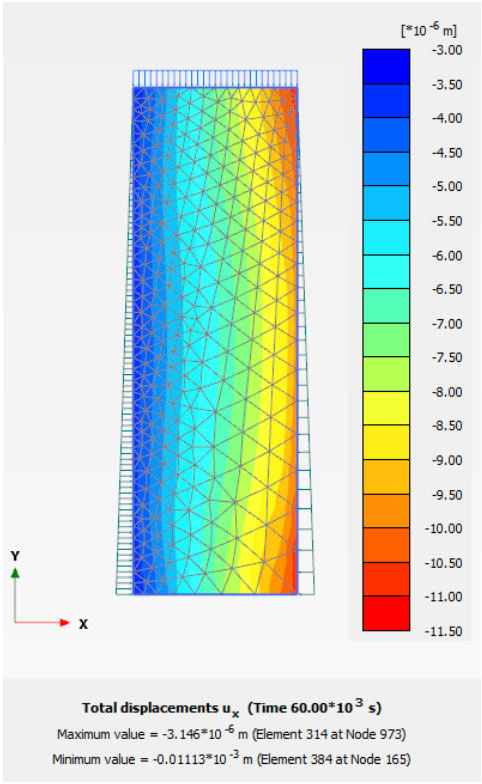

Figure 5.3 Displacements in the horizontal direction when the temperature is reduced from 0^{o}C to -1^{o}C. It is assumed that during this period, all soil water turned to ice and expansion of the sample took place.

In this stage, the water in the soil will freeze and an expansion of soil sample will take place. This process will cause some increase in the inner radius and the outer radius. However, the increase in inner radius in Stage 2 is less than the decrease in inner radius during Stage 1.

Stage 3: Temperature is reduced from -1^{o}C to -5^{o}C.

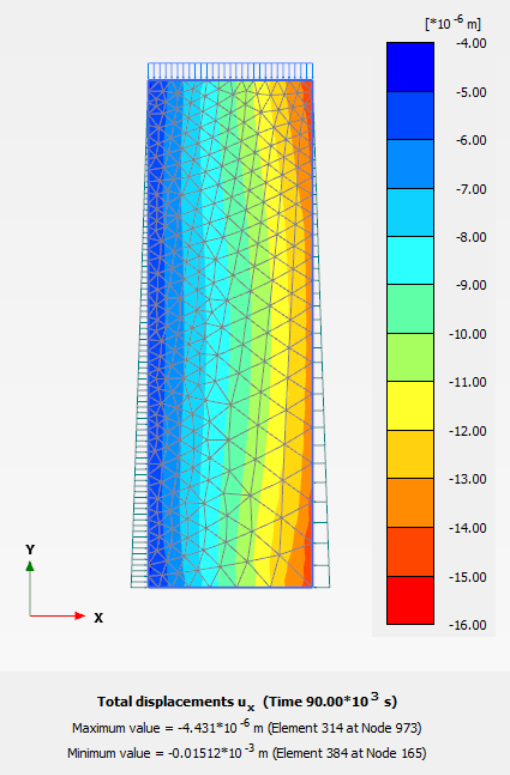

Figure 5.4 Displacement in the horizontal direction when the temperature is reduced from -1^{o}C to -5^{o}C

In this stage, the temperature is reduced from -1^{o}C to -5^{o}C. The soil with its water in frozen state continues to shrink further as the temperature is reduced. During this period, the ice in the soil voids also starts to shrink because the temperature was further reduced to -5^{o}C.

The plot shown below summarizes displacements of the inner radius during temperature changes.

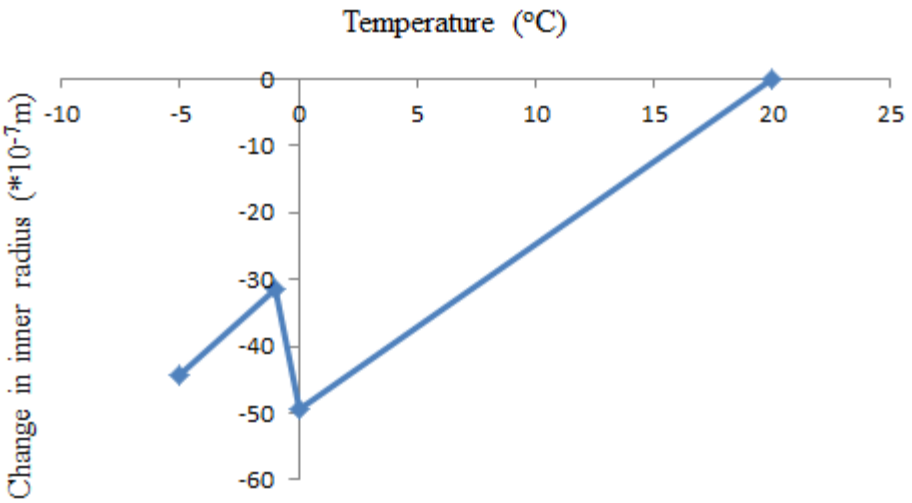

Figure 5.5 Summary of changes in inner radius as the temperature is reduced from 20°C to -5°C

The results shown in this figure provide some explanation for the observations made in the cold room experiments. Measured strains in the tube increase (i.e. the radius of the pile decreases) in the experiments, as the temperature decreases from 20°C to 0°C. Between 0°C and -1°C, there is a bump (i.e. an increase) in the experimental curve. Soil water freezes and the measured strains decrease (i.e. the radius of the pile increases) similar to the FE results. The trend in the remaining part of the cold room experiment is the same as shown in the FE results shown in Figure 5.5.

5.2 Analysis type 2

In the Type 2 analysis, temperature changes are reversed from the point where Type 1 analysis ended. Type 1 analysis was about the effect of decreasing temperatures and the minimum temperature was -5°C. In the Type 2 analysis, the temperature was increased from -5°C to the room temperature. Figure 5.6 shows the displacements in the horizontal direction when the temperature is increased from -5°C to 20°C.

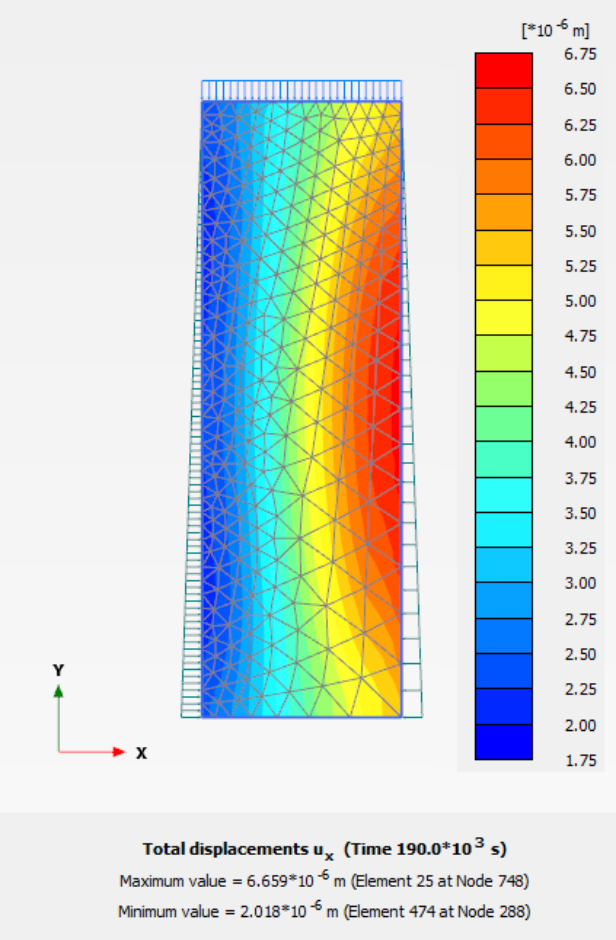

Figure 5.6 Displacement in the horizontal direction when the temperature is increased from -5^{o}C to 20^{o}C

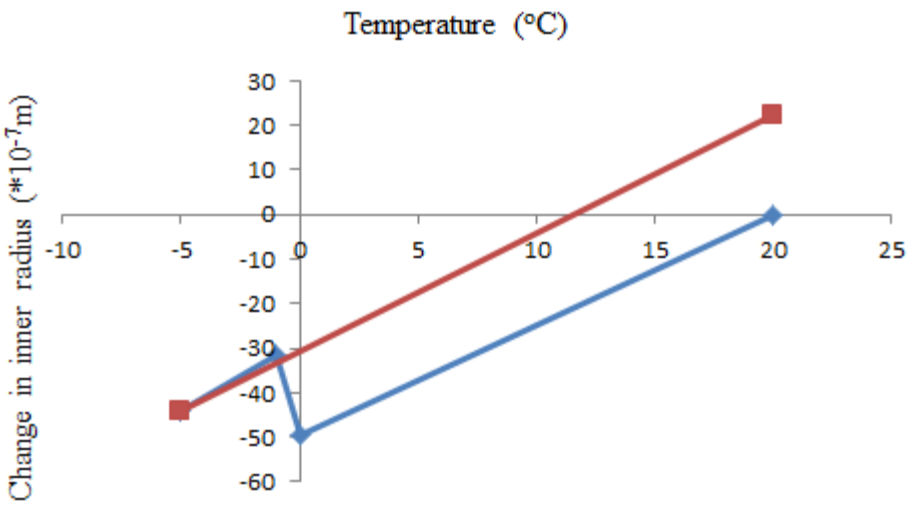

Figure 5.7 Summary of changes in inner radius as the temperature change from 20°C to -5°C first (the blue line) and then the temperature is increased again from -5°C to 20°C (red line)

The slopes of lines (blue or red) are dependent on the thermal properties and the elastic parameters used in the analyses. These parameters should be determined using laboratory experiments rather than the numbers used in the present FE calculations.

5.3 Analysis type 3

This type of analysis is related to reducing the temperatures down to -22°C following the Type 1 analysis. This analysis was needed because some of the pull-out tests on the model scale pile (Villeneuve, 2017) were conducted at -22°C outdoors in winter months. The finite element analysis gives the thermal effect on the mechanical behavior of the soil sample at that temperature.

Figure 5.8 shows the displacements in the horizontal direction when the temperature is decreased from -5°C to -22°C.

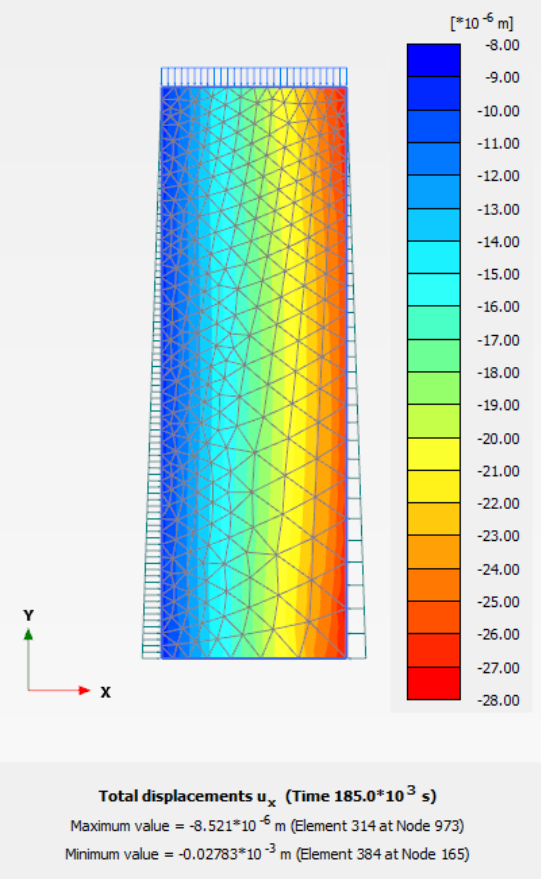

Figure 5.8 Displacements in the horizontal direction when the temperature is decreased from -5^{o}C to -22^{o}C

Between -5^{o}C and -22^{o}C the inner radius continues to decrease. In other words, the confining pressure acting on the pile would increase. Figure 5.9 can be used to determine the confining pressure acting on the pile at -22^{o}C.

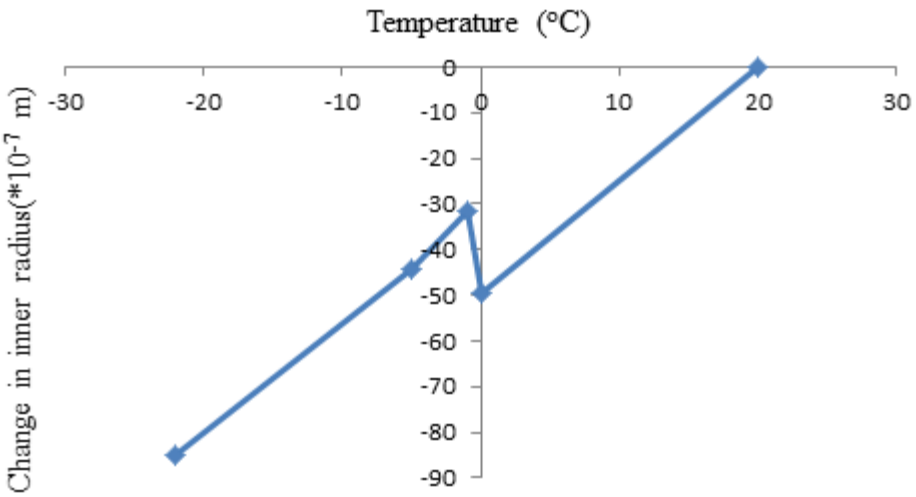

Figure 5.9 Summary of changes in inner radius as the temperature is reduced from 20^{o}C to -22^{o}C

CHAPTER SIX

ADFREEZE BOND STRENGTH COMPARISON BY TWO METHODS

In this chapter, the adfreeze bond strength measured by soil-pile interface testing method and pull-out testing method are compared. The interface tests were conducted as part of the present investigation. Villeneuve (2017) performed the model scale pull-out tests to measure the adfreeze strength at a model scale pile and frozen soil interface at the University of Ottawa.

6.1 Pull out test apparatus

The pile Villeneuve (2017) used in the pull-out tests is shown in Figure 6.1.

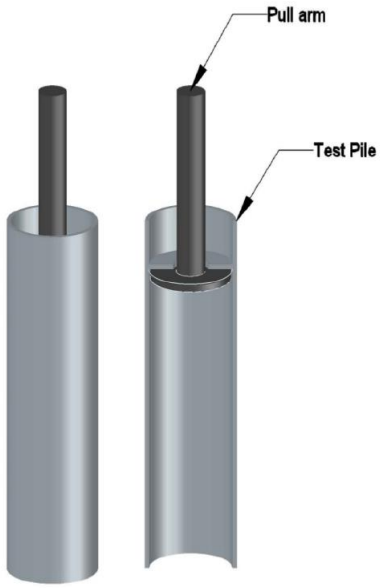

Figure 6.1 Test pile and pull arm front view on the left and cut view on the right (from Villeneuve, 2017). (Note that the soil and the container is not shown in this figure)

The pile radius is 57.2mm. The embedment depths of the pile in frozen soil are given later in Table 6.1.

Figure 6.2 shows the soil container which is a heavy steel box Villeneuve (2017) used in the pull-out tests. The interior dimensions of the soil container are 534mm×534mm×572mm (length, width, and height).

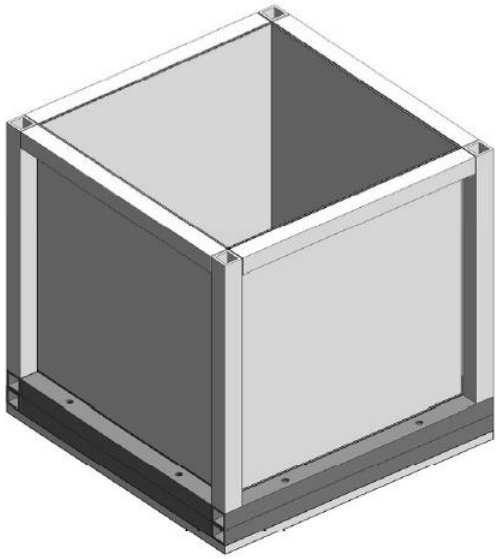

Figure 6.2 Soil container used in pull-out tests (Villeneuve, 2017)

6.2 Test settings

In the Villeneuve's experiments, the samples were frozen in a freezer in the lab in the summer and outside the building in the winter.

The lowest temperature the freezer could reach was -8^{o}C. In January and February 2015, the average outside temperature was -22^{o}C (Villeneuve, 2017).

The model scale pull-out experiments were done when the soil temperature was lower than -5^{o}C (Villeneuve, 2017).

According to Villeneuve (2017), the pull out rate was 0.1mm/min. The time, displacement and force were recorded by the data acquisition system of the testing machine. Thermistors were inserted in the soil sample. Thermistors and Raspberry PI were used to monitor the sample temperature. Foam insulation panels were used around the steel box (Figure 6.2) to keep the soil sample at the intended freezing temperatures.

6.3 Results of Villeneuve's pull-out tests

The results of pull-out tests using a model scale pile are given in Table 6.1. The embedded depth of the pile in soil was different in different tests.

Table 6.1 Data from the pull-out tests by Villeneuve (2017)

Test Name	Depth (mm)	Peak stress(kPa)	Residual stress(kPa)	Water content (%)	Dry density (kg/m^3)	Used or ignored
Pull out 1	533	553.42	N/A	17.10	N/A	Ignored
Pull out 3	533	N/A	218.51	13.10	N/A	Residual only
Pull out 4	521	635.36	N/A	14.10	N/A	Used
Pull out 5	429	N/A	N/A	13.65	2087.81	Ignored
Pull out 6	419	623.57	222.02	12.90	1943.55	Used
Pull out 7	428	517.19	159.62	11.61	2056.00	Used
Pull out 8	406	N/A	186.03	8.82	1912.64	Residual only
Pull out 9	406	497.16	129.05	10.30	1621.31	Used
Pull out 10	406	255.54	69.27	7.70	2102.79	Ignored
Pull out 11	406	519.03	146.41	9.50	1797.17	Used
Pull out 12	305	281.67	95.40	8.30	1904.62	Ignored
Pull out 13	305	318.14	99.47	9.87	1904.89	Used
Pull out 14	302	386.09	117.22	8.85	1694.99	Used

According to Villeneuve, some of his tests (6 out of 13) were not usable, because a manipulation issue had resulted in the rupture of the adfreeze bond before the beginning of the test. These tests were labeled as "Ignored" or "Residual only". The table provides the embedment depth of the pile (the second column), peak strength, residual strength, water

content of the soil, and the dry density. The peak strength was determined by dividing the maximum pull-out load by the surface area of the pile shaft. The peak stress is another term used by Villeneuve for the adfreeze bond strength of the soil-pile interface. Any resistance to pull-out at the toe of the pile was ignored because the pile was made of a steel pipe with an open end.

There are some inconsistencies in the data given in Table 6.1. For example, the water content in Test #9 is 10.3% and in Test #13 is 9.81%. According to the Proctor test results, the dry density in Test #9 is supposed to be larger than the dry density in Test #13. In contrary, Test #9 had a dry density of 1621.31 kg/m^3 which is much smaller than the dry density of 1904.89kg/m^3 in Test #13. Similar inconsistencies can be found with respect to "Peak stress" values when the results of Test #11 and Test #13 are compared.

6.4 Assessment of the confining pressure acting on the pile shaft in pull-out tests of Villeneuve (2017)

The literature review, as well as the experimental results reported in Chapter 4, show that adfreeze bond strength is (among other factors) a function of lateral normal stress (also referred to as confining pressure in this study) acting on the pile shaft. Villeneuve (2017) did not report the confining pressure (lateral normal stress) acting on the pile shaft. The confining pressure is an important factor in the determination of the shaft resistance. Its value has to be known. In the present study, an attempt has been made to estimate the confining pressure in Villeneuve's experiments.

Assuming that the horizontal cross-sectional shape of the steel box is circular and has the same area with the steel box, the radius of the circle would be 301.28mm. The magnitude of

the confining pressure acting on the pile shaft is influenced by three different processes. One of them is the shrinkage of the soil skeleton due to decreasing temperatures. Shrinkage continues above and below freezing temperatures as long as the temperature is decreasing. The second process that influences the magnitude of the confining pressure is the freezing of water. When the water in the voids of an unsaturated soil freezes, the volume of the soil mass tends to increase. The last process that affects the magnitude of the confining pressure in the pull-out tests is the soil compaction. In the present study, the soil around the pile was also compacted during the sample preparation as it is done in pull-out tests.

6.4.1 Effect of decreasing temperatures on shrinkage and expansion of soil mass

During decreasing temperatures, soil particles, as well as soil skeleton, would shrink. This process continues irrespective of the value of temperature whether it is above or below the freezing temperature of water. When water in the voids of the soil freezes, it results in expansion. As a result of these two processes, i.e. shrinkage and expansion, the confining pressure acting on the pile shaft would change. In order to determine the changes in the confining pressure, the amount of shrinkage, as well as expansion due to decreasing temperatures including below freezing temperatures, need to be determined. This is done by an experiment in the laboratory as described below.

The modified direct shear machine is used to assess the shrinkage and expansion of the soil. Two experiments were conducted. There was no applied load on the soil samples. Deformation of the soil samples was allowed to take place freely when the temperature is changed in the test chamber. In the first type of experiments, to assess the effect of water content on shrinkage and freezing expansion, two experiments were conducted. The soil samples had 11% and 13% gravimetric water contents, respectively. Both soil samples had

2025 kg/m^3 dry density. The freezing expansions were 0.06204mm and 0.1276mm at 11% and 13% gravimetric water contents as shown in Figure 6.3 and Figure 6.4. During the initial part of the experiments, the sample height decreased due to the shrinkage caused by temperature reduction from the room temperature to the freezing temperature. Once the water started to freeze, the sample height began to increase.

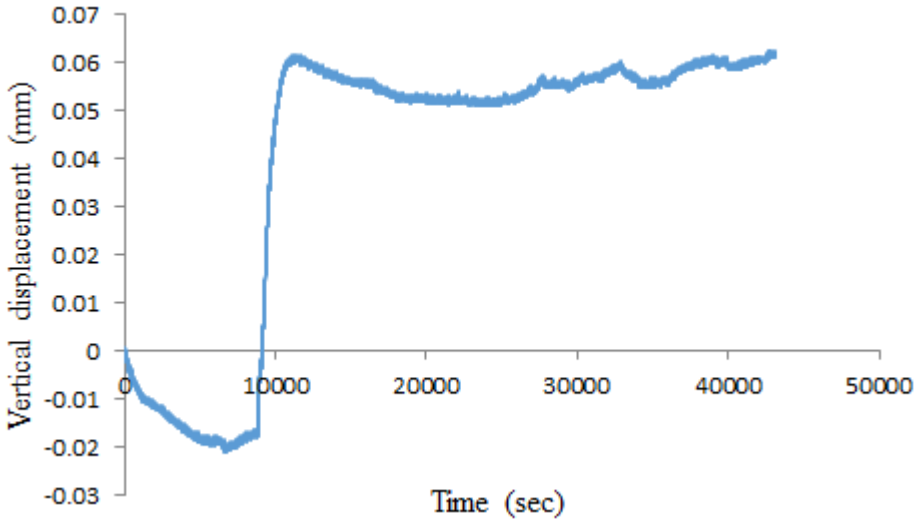

Figure 6.3 Shrinkage and freezing expansion at 11% water content

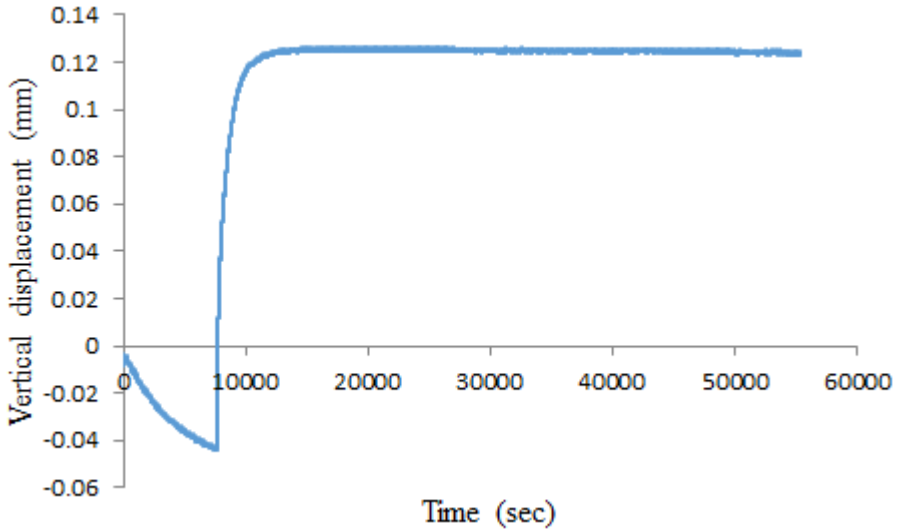

Figure 6.4 Shrinkage and freezing expansion at 13% water content

The relationship between water content and shrinkage is given in Figure 6.5.

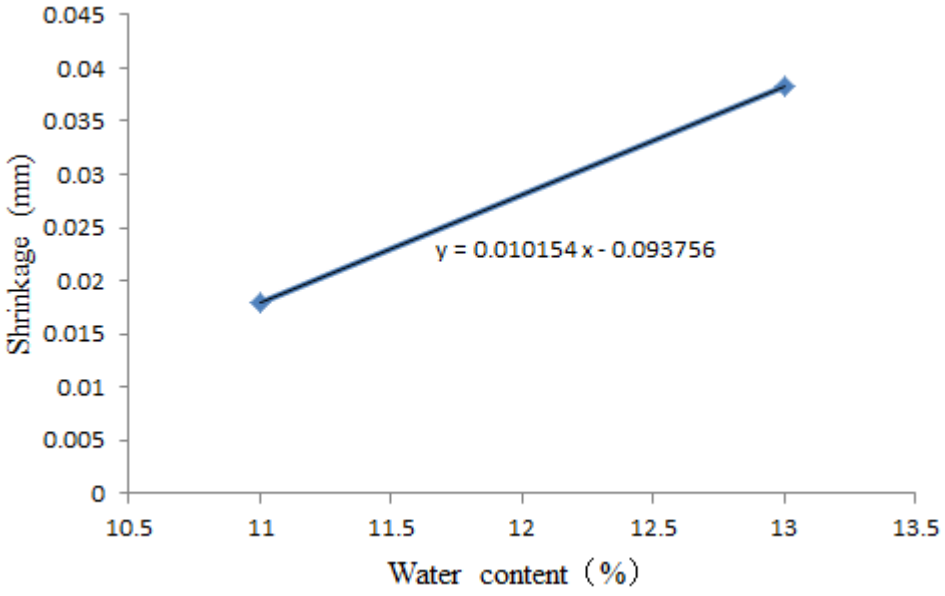

Figure 6.5 Shrinkage as a function of water content

The relationship between water content and freezing expansion is given in Figure 6.6. As would be expected, freezing expansion increases as the water content increases. It should be noted that the coefficient of thermal expansion can be determined by dividing the freezing expansion by the height of the soil sample.

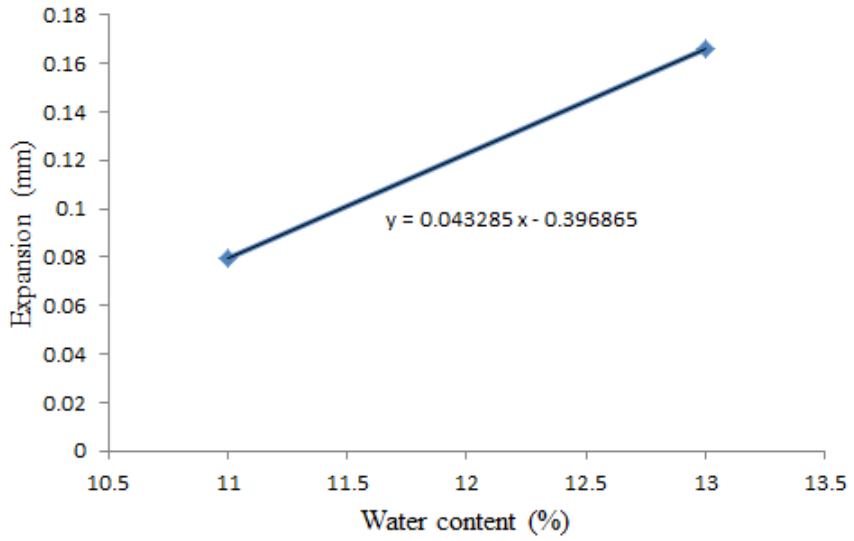

Figure 6.6 Expansion due to freezing as a function of water content

In the second type of experiments, to assess the effect of dry density alone on shrinkage and freezing expansion, two experiments were conducted. The dry densities of the two soil samples were 1989.2 kg/m^3 and 2058.4 kg/m^3, respectively. Both soil samples had 13% gravimetric water content. The shrinkage and freezing expansions are shown in Figure 6.7 and Figure 6.8.

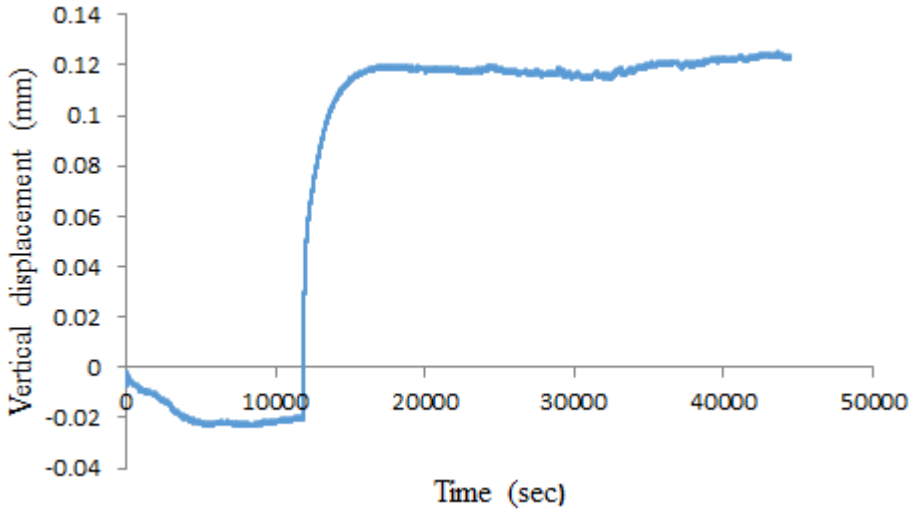

Figure 6.7 Shrinkage and freezing expansion at a dry density of 1989.2kg/m^3 and 13% water content

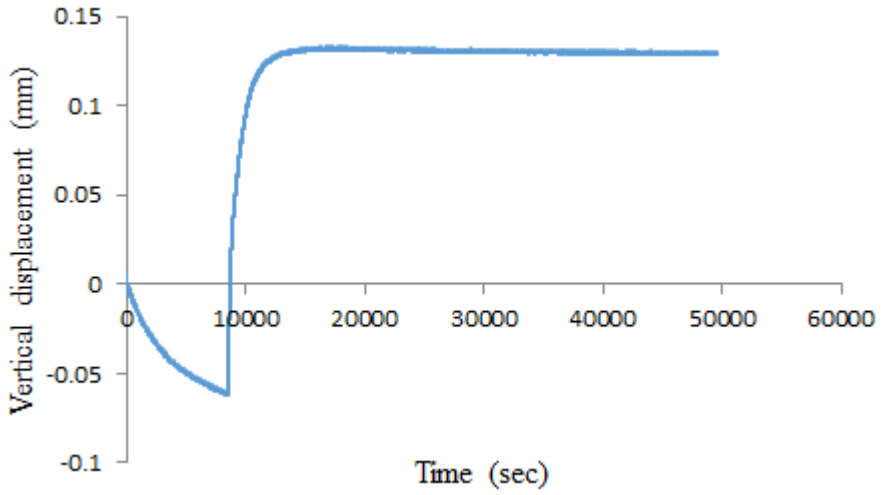

Figure 6.8 Shrinkage and freezing expansion at a dry density of 2058kg/m^3 and 13% water content

Figure 6.9 shows the relationship between dry density and amount of shrinkage.

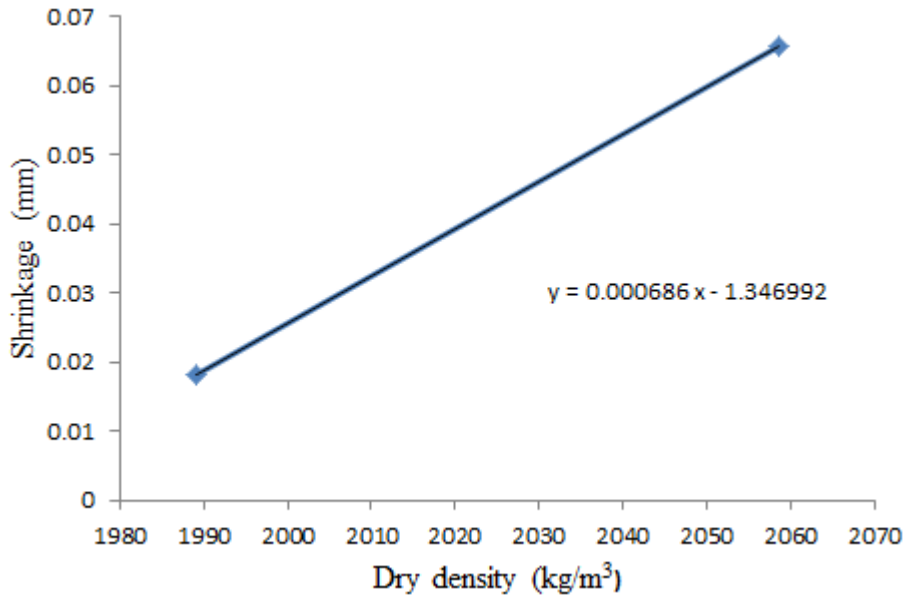

Figure 6.9 Relationship between shrinkage and dry density

Figure 6.10 shows the relationship between dry density and freezing expansion. As shown in the figure, the freezing expansion increases with increasing dry density.

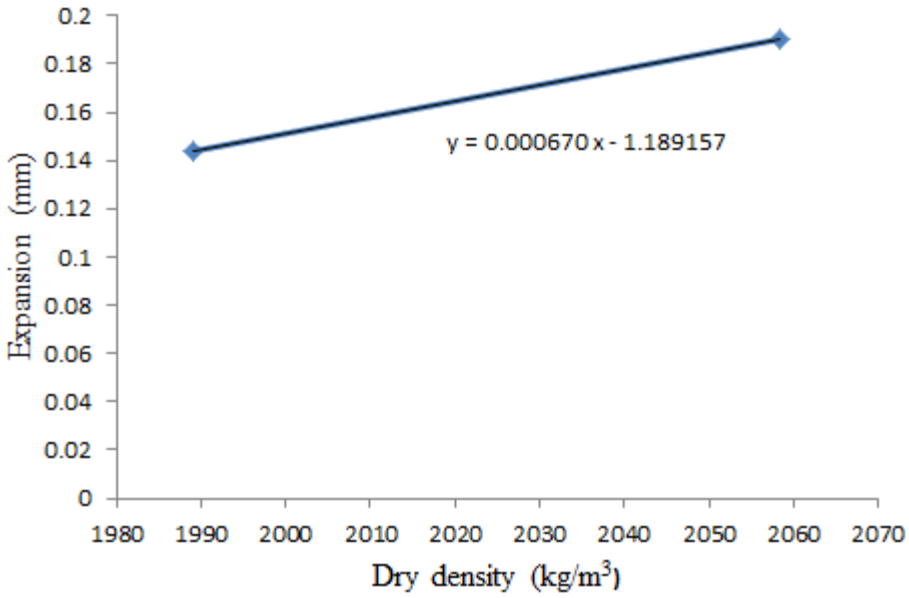

Figure 6.10 Relationship between dry density and freezing expansion

Within the range of dry densities shown in Figure 6.10, the influence of the change in dry density has an insignificant effect on the freezing expansion compared to the effect of a change in water content.

6.4.2 Estimation of confining pressure in cold room experiment of the present study

Before an attempt is made to determine the confining pressure acting on the pull-out experiments of Villeneuve, a possibility of using a simple method for the calculation of the confining pressure in the cold room experiment of the present study is investigated. In this simple method, the following steps are used. In order to compare the estimated results, the measured data from the cold room experiment are utilized.

Step 1:

In the cold room experiment, the average length of the soil in the radial direction is 100mm. Let us assume that a representative linear soil element of this length in the radial direction (with 1 mm^2 cross-sectional area) is subjected to temperature changes. As shown in Figure

6.11, the changes in temperature ranging between room temperature of 20°C and 0°C, will cause the element to change its length. Consequently, the outside boundary of the soil sample will move to a new location as shrinkage takes place. The magnitude of the shrinkage can be calculated using the experimental data shown in Figure 6.5. The data shown in Figure 6.5 was obtained from a sample of 15mm thick. For 100mm long soil element in the cold room experiment the amount of shrinkage would be 0.1196mm. The corresponding axial strain will be 0.001196.

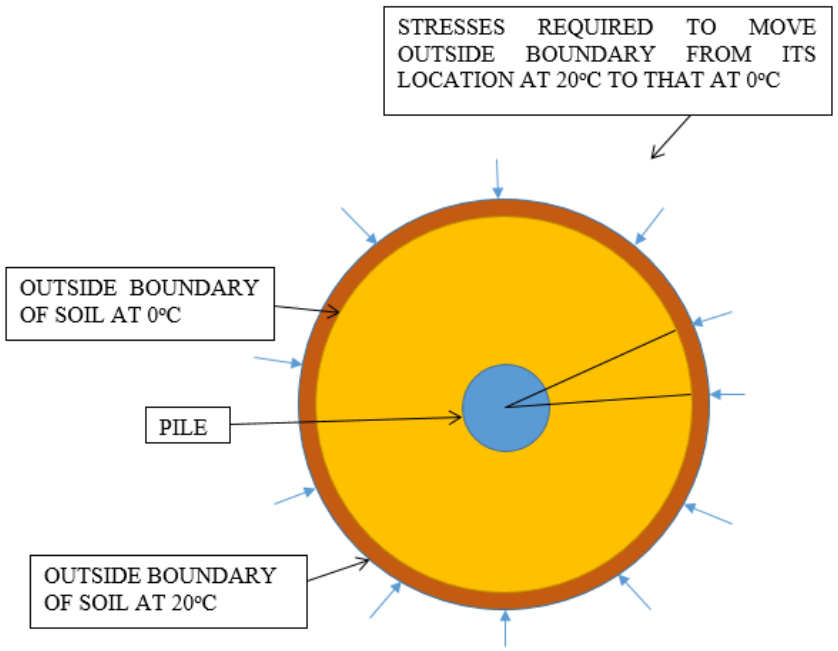

Figure 6.11 Illustration of soil shrinkage and the stress required to bring the outside boundary from its location at 20°C to that at 0°C

Step 2:

This step starts from an undeformed soil sample. A uniformly distributed normal stress is applied at the outer boundary of the soil as shown in Figure 6.11. The objective of this step is to find the magnitude of the normal stress that will cause same amount of soil deformation

that is caused by shrinkage. The amount of shrinkage as well as the magnitude of the axial strain in the 100 mm long soil element is already calculated in Step1. Therefore, the normal stress divided by the deformation modulus should be equal to the axial strain. It is assumed that the soil behavior is elastic and a range of values can be estimated by a literature survey. Most textbooks on foundation engineering provide elastic moduli for various types of soils. For dense sand, the values of elastic modulus range approximately between 50000kPa and 150000kPa. In this step, three values (80000, 100000, and 120000kPa) are chosen arbitrarily to see what effect they would have on the calculation of normal stress that should be applied on the outer boundary of soil sample. Estimated values of normal stress are given below.

Normal stress = 96kPa for elastic modulus = 80000kPa

Normal stress = 120kPa for elastic modulus = 100000kPa

Normal stress = 144kPa for elastic modulus = 120000kPa

Step 3:

In this step, the confining pressure acting on the PVC tube in the cold room experiment is calculated from the results obtained in Step 2 for the normal stress which needs to be applied at the outer boundary. Force equilibrium requires that

(Confining pressure acting on the PVC tube) $\times$ (Circumference of PVC tube times the soil depth) = (Normal stress acting on the outside boundary of soil) $\times$ (Circumference of outside boundary of soil times the soil depth)

These calculations give the following estimated confining pressures.

Confining pressure acting on PVC tube = 288kPa for Normal stress = 96kPa

Confining pressure acting on PVC tube = 360kPa for Normal stress = 120kPa

Confining pressure acting on PVC tube = 432kPa for Normal stress = 144kPa

These estimated confining pressures are based on arbitrarily chosen elastic modulus values from the literature survey.

Another approach for estimating the elastic modulus would be to use equations developed by various researchers. For example, the following table is taken from the website of Professor Sture, Colorado State University shows some equations developed by Vermeer & Schanz and NTNU. These equations are based on drained triaxial tests on sand.

Table 6.2 Equations of the elastic modulus of sand at a stress level 50% of peak strength (from A short course on Computational Geomechanics, 2004 by Prof. Stein Sture, University of Colorado at Boulder.)

	Vermeer and Schanz	NTNU
Loose or silty:	$\frac{E_{50}}{p^{ref}} \approx 150\sqrt{\frac{\sigma_x^{'}}{p^{ref}}}$	$\frac{E_{50}}{p^{ref}} \approx 100\sqrt{\frac{\sigma_x^{'}}{p^{ref}}}$
Dense and clean:	$\frac{E_{50}}{p^{ref}} \approx 500\sqrt{\frac{\sigma_x^{'}}{p^{ref}}}$	$\frac{E_{50}}{p^{ref}} \approx 600\sqrt{\frac{\sigma_x^{'}}{p^{ref}}}$

$p^{ref} = 100kPa$

In order to use these equations, one needs to know the confining pressure acting on the soil sample in triaxial tests. This creates a problem for the use of these equations in the estimation of confining pressure acting on the PVC pipe. Soil stiffness varies depending on stress level. Stress level which includes the confining pressure acting on the PVC pipe cannot be used to determine the elastic modulus for the purpose of using this simple method. There are many constitutive equations describing the stress-strain-strength behavior of soils

(Chen and Saleeb, 1982). They should be used in the calculations of confining pressure acting on the PVC pipe.

At this stage of the investigation, pursuing a simple approach to determine the confining pressure during temperature changes, including the freezing temperature, is discontinued.

The method is too crude to analyze the cold room experiment of the present study. Therefore, the use of this simple method is not extended to the analysis of pull-out tests of Villeneuve (2017).

6.4.3 Assessment of confining pressure acting on the pile shaft in pull-out tests of Villeneuve (2017)

The method described in this section makes use of the cold room experiments conducted in the present study. This method is different than the one described in Section 6.4.2. In these calculations, the following steps are used. It is assumed that the confining pressure acting on the pile shaft in pull-out tests is the same as measured in the experiment described in Chapter 3 of the present study. In other words, temperature changes and compaction have the same effect on the confining pressure measured in the present study and pull-out tests of Villeneuve (2017). For the estimation of adfreeze bond strength in the pull-out tests, the experimental data from Chapter 4 are utilized.

6.5 Estimation of adfreeze bond strength in two pull-out tests

The adfreeze strength in two pull-out tests of Villeneuve (2017) is estimated as described in the following. The selection of these two tests was based on the water content in the cold room experiment of present study was very close to the water contents in two pull-out tests.

6.5.1 Analysis of pull out Test #9

In the pull-out Test #9, the peak stress (adfreeze strength) was 497.16 kPa. The test was carried out during summer months. The temperature in the cold room was -7^{o}C. The water content of the soil was 10.3%. Soil density (1621.31 kg/m^{3}) was unusually low. Following steps are followed in the calculations.

Step 1: Determine the adfreeze strength of the interface for soil sample at 10.3% water content as a function of normal stress acting on the interface. Use the results of the adfreeze strength tests corresponding to water contents at 11% and 9% (see Figure 4.15). The values of adfreeze bond strength corresponding to normal stress values of 25 kPa and 80 kPa can be used. The following equation is obtained for the relationship between adfreeze bond strength and normal stress for water content equal to 10.3%.

$$\tau_{adf} = 0.9964 \times \sigma_n + 48.79 \qquad \text{Eq. 6.1}$$

where τ_{adf} is the adfreeze bond strength and σ_n is the normal stress.

(Note: Unit of stress in Eq. 6.1 is kPa)

Step 2: Make use of Figure 3.10 to determine the confining pressure at -7^{o}C. The magnitude of confining pressure is 550kPa.

Step 3: Use the confining pressure determined in Step 2 to replace σ_n in Eq. 6.1. The adfreeze strength determined from this equation is τ_{adf} = 597kPa. It is noted that Eq. 6.1 is a linear approximation to the test data. The range of normal stress used in the adfreeze experiments is between 25kPa and 80kPa. It is possible that a linear trend line is not

representative of the interface behavior at much larger normal stress values. The following step is used to see what effect would be on τ_{adf} if a nonlinear trend line were used.

Step 4: This step makes use of experimental data of Choi et al. (2014) shown in Figure 6.12.

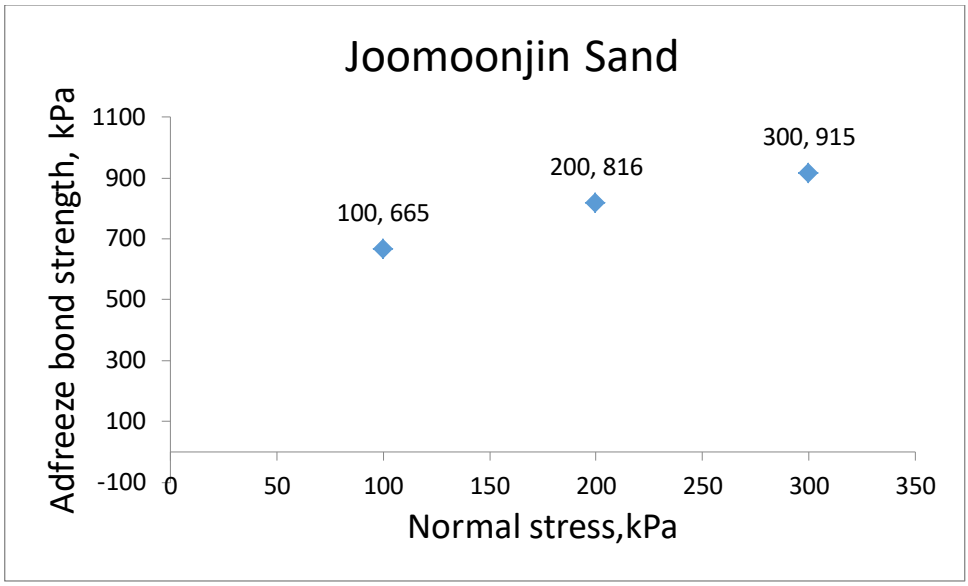

Figure 6.12 Adfreeze bond strength versus normal stress for Joomoonjin Sand (Choi et al. 2014)

The confining pressures used in this figure range between 100kPa and 300kPa. The purpose of using the data shown above is to determine the adfreeze strength of Joomoonjin Sand at a normal stress out of the range of normal stress used in the actual experiments. In order to determine the effect of nonlinearity in the data, two kinds of trend lines are used. The first one is a linear trendline (Figure 6.13). The second one is a second order polynomial trend line (Figure 6.14).

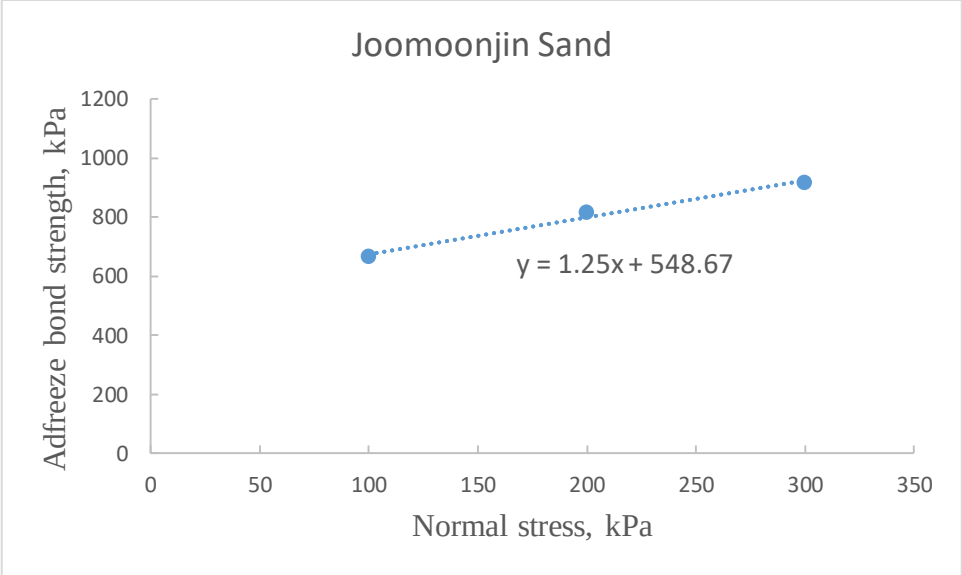

Figure 6.13 A linear trendline for adfreeze bond strength and normal stress for Joomoonjin Sand (Choi et al. 2014)

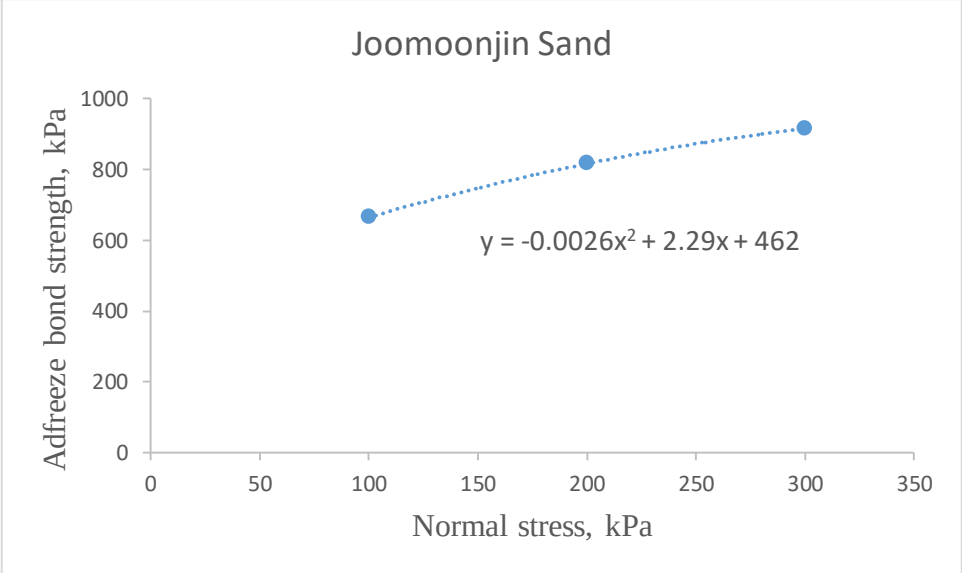

Figure 6.14 A second order polynomial trendline for adfreeze bond strength and normal stress for Joomoonjin Sand (Choi et al. 2014)

Using a linear trendline gives adfreeze strength at 550 kPa normal stress equal to

τ_{adf} = 1.25(550) +548.67 =1236kPa

The polynomial trendline gives adfreeze bond strength at 550 kPa normal stress equal to

$\tau_{adf} = -0.0026(550)^2 + 2.29(550) + 462 = 935\text{kPa}$

Using a polynomial trend line gives much lower adfreeze bond strength than the value calculated by a linear trend line. The amount of reduction, as a ratio, is 935/1236=0.756.

Step 5: Use the reduction factor 0.756 determined in Step 4, in the calculation of the adfreeze strength of the Cornwall Sand. In other words, multiply the adfreeze strength τ_{adf} = 597kPa determined in Step 1, by the reduction factor of 0.756: The new estimate of the adfreeze bond strength at σ_n = 550kPa becomes $\tau_{adf} = 597 \times 0.756 = 452\text{kPa}$.

Pull-out Test #9 by Villeneuve has a measured value of 497kPa. The difference can be attributed to many factors.

6.5.2 Analysis of pull out test #7

Figure 6.15 is the confining pressure variation caused by compaction and temperature change from room temperature 20^{o}C to -22^{o}C. From the figure, we can find the confining pressure acting on pile shaft, which is 650kPa due to compaction of the soil, soil weight and temperature change at -22^{o}C.

.

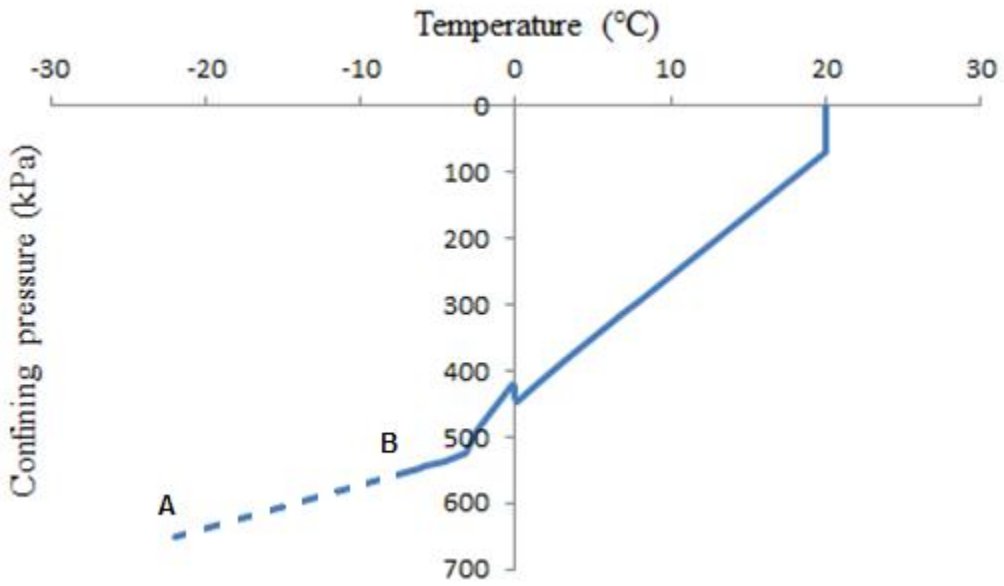

Figure 6.15 Confining pressure variation with compaction and temperature-bigger tube embedded in soil

From Figure 4.15 in Chapter four, the relationship between normal stress and peak strength at 11% water content is y=1.2194x+61.032 where "x" means the normal stress and "y" means the peak strength. So if "x" is equal to 650 kPa, then "y" will be 853.642 kPa. Therefore, adfreeze bond strength in pull out test #7 done by Villeneuve (2017) is 853.642 kPa by using the cold room experiment analysis.

Choi et al. 2014 performed cold room experiments on an interface between Joomoonjin Sand and an aluminum plate to determine the adfreeze bond strength. It is possible that a linear trendline is not representative of the interface behavior at very larger normal stress values. To get the adfreeze bond strength at a high magnitude of normal stress, a reduction coefficient is used on the estimated adfreeze strength based on a linear trend line. The calculation of the reduction factor is described next. The following analysis also provides the final value of the estimated adfreeze strength.

If the relationship between normal stress and peak strength is linear, the equation between them will be y=1.25x+548.67 as shown in Figure 6.13 where "x" means the normal stress and "y" means the peak strength. According to the equation in Figure 6.13, when the normal stress is 650kPa, the peak strength will be 1361.17 kPa.

If the relationship between normal stress and peak strength is polynomial, the equation between them will be $y = -0.0026x^2 + 2.29x + 462$ as shown in Figure 6.14 where "x" means the normal stress and "y" means the peak strength. According to the equation in Figure 6.14, when the normal stress is 650 kPa, the peak strength will be 852kPa.

So the amount of reduction, as a ratio, is 852/1361.17=0.626. If we use this reduction coefficient factor on the peak strength in pull out test #7 performed by Villeneuve (2017), the adfreeze bond strength in the pull-out test will be 534.71kPa by using the cold room experiment analysis. Pull-out Test #7 by Villeneuve has a measured value of 517.19kPa. The difference can be attributed to many factors.

6.6 Conclusions of Analysis

Analyses of two of pull out tests suggest that the confining pressure acting on the pile shaft needs to be known for an estimate to be made for the adfreeze bond strength from the interface experiments.

CHAPTER SEVEN

SUMMARY AND CONCLUSIONS

The solar panels installed in the region of Cornwall, Ontario are supported by piles. For the design of these piles, it is necessary to determine the adfreeze bond strength of the interface between the Cornwall sand and piles. Villeneuve (2017) performed pull-out tests using a model scale pile in Cornwall sand to determine the adfreeze bond strength. It is well known that the adfreeze bond strength is a function of normal stress acting on the interface. In Villeneuve's experiments, normal stress was not measured.

One of the objectives of the present study is to estimate the magnitude of the normal stress acting on the pile shaft in the pull-out tests of Villeneuve. This objective is achieved by running an experiment in a cold room. Similar to Villeneuve's experiments, a 100mm diameter pile is used in a cold room experiment. The soil was Cornwall sand and it was compacted the same way as in pull-out tests. Magnitudes of hoop strain were recorded as a function of temperature. Later, confining pressures were determined from measured strain at each temperature.

In the present study, a set of interface tests is conducted to determine the adfreeze bond strength of an interface between Cornwall Sand and a steel plate. These tests are conducted using a modified direct shear apparatus. An insulated chamber is built around the direct shear box, the soil sample and the interface plate. It was possible to reduce the temperature in the test chamber from $23^{o}C$ to $-5^{o}C$ and maintain it at that temperature until the end of testing. To determine the adfreeze bond strength nine interface tests are conducted. In these tests, the soil samples have a gravimetric water content of $9\%, 11\%$, and 13%. The soil

samples are subjected to 25kPa, 45kPa and 80kPa normal stress at each magnitude of water content. Experimental data show that the relationship between the normal stress and the adfreeze bond strength is almost linear within the range of normal stresses applied in these tests.

The adfreeze bond strength data measured by soil-pile interface testing method and pull-out testing method are compared. By making use of Figure 3.10, it is estimated that the confining pressure acting on the pile shaft in pull out test #7 was 650 kPa and in pull out test #9 was 550kPa.

The experimental data of Choi et al. (2014) is analyzed. It is possible that a linear trend line is not representative of the interface behavior at very larger normal stress values. In order to determine the effect of nonlinearity in the data, two kinds of trend lines are used. The first one is a linear trend line (Figure 6.13). The second one is a second order polynomial trend line (Figure 6.14). It is found that using a polynomial trend line gives lower adfreeze bond strength than the value calculated by a linear trend line. The amount of reductions, as a ratio, is 0.756 in pull out test #9 and 852/1361.17=0.626 in pull out test #7.

Making use of the adfreeze bond strength reduction ratio for very large normal stresses, it is determined that the adfreeze bond strength measured in the interface test is 534.71 kPa at 11% soil water content and 650kPa normal stress. This number is very close to the adfreeze bond strength of 517.19 kPa in the pull-out test #7 by Villeneuve at 11.61% water content.

The same method described above is used to compare the adfreeze bond strength measured in the interface test and the pull-out test #9. In the pull-out test #9, the water content was 10.3% and the temperature was -7^{o}C. Adjustments were made for the differences in the

water content and temperature to calculate the normal stress to be used in the analysis of data. The adfreeze bond strength determined from the interface tests was 452kPa. This value compares well with the adfreeze bond strength 497.2kPa measured in pull-out test# 9.

An attempt made to develop a simple method to estimate the confining pressures acting on the pile shaft in the pull-out tests of Villeneuve was not successful. The conclusion of that effort was that a nonlinear stress-strain relation representing the soil behavior in both unfrozen and frozen states needs to be used in the analysis.

REFERENCES

ACIA. 2005. Arctic climate impact assessment: Scientific report. Cambridge: Cambridge University Press. 1042 p.

Adamson, B., Claesson, J. and Eftring, B., 1973. Slab-on-grade. Foundation depth. National Swedish Institute for Foundation Research, Rep. R40.

Aldaeef A.A. and Rayhani M.T. 2017. Adfreeze Strength and Creep Behaviour of Pile Foundations in Warming Permafrost. Advances in Analysis and Design of Deep Foundations, Sustainable Civil Infrastructures: 254-264.

Aldaeef A.A. and Rayhani M.T. 2016. Evolution of Adfreeze Strength of Pile Foundations in Warming Permafrost. Canadian Geotechnical Conference, GEO-VANCOUVER 2016.

Andersland, O.B., & Ladanyi, B.1994. *An Introduction to Frozen Ground Engineering*. Chapman & Hall, Inc., New York, NY.

Andersland, O.B., & Ladanyi, B. 2004. *Frozen Ground Engineering*. John Wiley & Sons.

Andersland, O.B., & Anderson, D. 1978. Geotechnical Engineering for Cold Regions. McGraw-Hill Inc.

Andersland O.B., Alwahhab M.R. 1983. Lug behavior for model steel piles in frozen sand. Permafrost, Proceedings 4th International Conference, National Academy Press, Washington, DC 1983 (pp. 16-21).

Ashby, M.F., and Frost, H.J. 1975. Deformation mechanism and maps applied to the creep of elements and simple inorganic compounds. Chap. 11 in Frontiers in Materials Science, ed. L. E. Murr and C. Stein. New York: Marcel Dekker, pp. 391-419.

Bowles, J.E. 1996, Foundation analysis and design 5th ed., McGraw-Hill, New York, pp. 472-533.

Brown, J. and Haggerty, C. 1998. Permafrost digital databases now available. Eos, Transactions American Geophysical Union, 79(52), pp.634-634.

Camill, P. 2005. Permafrost thaw accelerates in boreal peatlands during late-20th century climate warming. Climatic Change 68(1-2):135 – 152.

Chen, W.F. and Saleeb, A.F., 1982. Constitutive Equations for Engineering Materials,< ol. 1. Elasticity and Modeling.

Choi, C., Lee, J., Kim, T.H. and Ko, S.G. 2014. Design parameters of micro piles in permafrost sandy ground. IWM, Krakow, Poland.

Crory, F.E. 1973. Settlement associated with the thawing of permafrost. In North Am. Contrib., 2nd Int. Conf. on Permafrost, Yakutsk, USSR. Washington, D.C.: National Academy of Sciences, pp. 599-607.

Crory, F.E. 1966. Pile foundations in permafrost. In Permafrost: Proceedings of North American Contribution to First International Conference on Permafrost (pp. 467-476).

Fang, H-U. 1991, Foundation engineering handbook, Van Nortrand Reinhold, New York, pp. 735-749.

Farouki, O. 1992. European Foundation Designs for Seasonally Frozen Ground. U.S. Army Cold Regions Research and Engineering Laboratory Monograph 92-1.

Giraldo, J., Rayhani, M.T. 2013. Influence of fiber-reinforced polymers on pile–soil interface strength in clays. Adv. Civ. Eng. Mater. 2(1), 1–17. doi:10.1520/ACEM20120043. ISSN2165-3984

Glen, J.W. 1955. The creep of polycrystalline ice. Proc. R. Soc. Lond. A. 1955 Mar 22;228(1175):519-38.

Goughnour, R.R., and O.B. Andersland. 1968. Mechanical properties of a sand-ice system. J. Soil Mech. Found. Div. ASCE 94(SM4): 923-50.

Haynes F.D. 1978. Strength and deformation of frozen silt. Proceedings of the Third International Conference on Permafrost, Edmonton, Alberta, Canada 1978 (Vol. 1, pp. 655-661).

Haynes F.D., Karalius J.A. 1977. Effect of temperature on the strength of frozen silt. Cold Regions Research and Engineering Laboratory, Hanover, NH; 1977 Feb.

Heydinger A.G. Piles in permafrost. 1987. Journal of Cold Regions Engineering. 1(2):59-75.

Hong E, Perkins, R. and Trainor S. 2014. Thaw Settlement Hazard of Permafrost Related to Climate Warming in Alaska. Arctic, Vol.67, No.1: 93-103.

Hooke, R. LeB., B. B. Dahlin, and M. T. Kauper. 1972. Creep of ice containing dispersed fine sand. J. Glaciol. 11(63): 327-36.

Hult, J. A. H. 1966. Creep in Engineering Structures. Waltham, Mass.: Blaisdell.

Jorgenson, M.T., Racine, C.H., Walters, J.C., and Osterkamp, T.E. 2001. Permafrost degradation and ecological changes associated with a warming climate in central Alaska. Climatic Change 48(4):551 – 579.

Jorgenson, M.T., Romanovsky, V., Harden, J., Shur, Y., O'Donnell, J., Schuur, E.A.G., Kanevskiy, M., and Marchenko, S. 2010. Resilience and vulnerability of permafrost to climate change. Canadian Journal of Forest Research 40(7):1219 -1236.

Jorgenson, M.T., Yoshikawa, K., Kanveskiy, M., Shur, Y., Romanovsky, V., Marchenko, S., Grosse, G., Brown, J., and Jones, B.H. 2008. Permafrost characteristics of Alaska. In:

Kane, D.L., and Hinkel, K.M. Ninth International Conference on Permafrost, 29 June – 3 July 2008, Fairbanks, Alaska. 121 – 122.

Konrad J.M. and Morgenstern N.R. 1984. Frost heave prediction of chilled pipelines buried in unfrozen soils. Canadian Geotechnical Journal. 21(1):100-15.

Ladanyi B. 1995. Frozen soil-structure interfaces. Studies in Applied Mechanics 1995 Jan 1 (Vol. 42, pp. 3-33). Elsevier.

Ladanyi, B., & Theriault, A. 1990. A study of some factors affecting the adfreeze bond of piles in permafrost. In Proc. of Geotechnical Engineering Congress GSP (Vol. 27, pp. 213-224).

Ladanyi, B. 1983. Shallow foundations on frozen soil: Creep settlement. J. Geotech. Eng. ASCE 109(11): 1434-48.

Ladanyi, B., and Johnston, G. H. 1974. Behavior of circular footings and plate anchors embedded in permafrost. Canadian Geotechnical Journal, 11, pp. 531-553.

Ladanyi, B. 1972a. An engineering theory of creep of frozen soils. Canadian Geotechnical Journal, 9(1):63-80.

Linell, K.A., and C. W. Kaplar. 1966. Description and Classification of Foundations in Areas of Deep Seasonal Frost and Permafrost. U.S. Army Cold Regions Research and Engineering Laboratory Special Report 80-34.

Linell, K.A., Lobacz, E.F. Design and construction of foundations in areas of deep seasonal frost and permafrost (No. CRREL-SR-80-34). Cold Regions Research and Engineering Lab., Hanover, NH.

Linell, K.A., Johnston, G.H. 1973. Engineering design and construction in permafrost regions: a review. Nat. Res. Counc. Can. 13848, 553–575 (1973)

Linell, K. A. and Lobacz, E. F. 1980, Design and construction of foundations in areas of deep seasonal frost and permafrost, Special Report of Cold Regions Research Engineering Laboratory, U.S. Army, pp. 80-134.

Maksimovg, H. 1967. Time of natural freezing around piles driven into permafrost. Osnovaniya Fundamenty I Mekhanika Gruntov, No. 3, pp. 12–14

Mellor, M. 1979. Mechanical properties of polycrystalline ice. In Physics and Mechanics of Ice: IUTAM Symp., Copenhagen, ed. P. Tryde. Berlin: Springer- Verlag, pp. 217-45.

Morgenstern, N.R., Roggensack, W.D., and Weaver, J. S.1980. The behavior of friction piles in ice and ice-rich soils. Canadian Geotechnical Journal, 17, pp. 405-415.

Nelson, F.E., Anisimov, O.A., and Shiklomanov, N.I. 2002. Climate change and hazard zonation in the circum-Arctic permafrost regions. Natural Hazards 26(3):203 – 225.

Nixon, J. F., & McRoberts, E. C. 1976. A design approach for pile foundations in permafrost. Canadian Geotechnical Journal, 13(1), 40-57.

Nottingham, D., and A. B. Christopherson. 1983. Driven piles in permafrost: State of the art. In Proc. 4th Int. Conf. on Permafrost, Fair-banks, Alaska. Washington, D.C.: National Academy Press, pp.928-33.

Odqvist, F. K. G. 1966. Mathematical theory of creep and creep rupture. Clarendon Press, Oxford, 168 p.

Osterkamp, T.E., Jorgenson, M.T., Schuur, E.A.G., Shur, Y.L., Kanevskiy, M.Z., Vogel, J.G., and Tumskoy, V.E. 2009. Physical and ecological changes associated with warming permafrost and thermokarst in interior Alaska. Permafrost and Periglacial Processes 20(3):235 – 256.

Parameswaran, V. R. 1978. Adfreeze strength of frozen sand to model piles. Canadian Geotechnical Journal, 15(4), 494-500.

Parameswaran, V. R. 1979. Creep of model piles in frozen soil. Canadian Geotechnical Journal, 16(1), 69-77.

Parameswaran, V. R. 1981. Adfreeze strength of model piles in ice. Canadian Geotechnical Journal, 18(1), 8-16.

Parameswaran, V. R. 1986. Bearing capacity calculations for piles in permafrost. Proceedings of the Fourth International Conference, Anchorage, Alaska, Cold Regions Engineering, 751-759.

Patterson, D. E., and M. W. Smith. 1983. Measurement of unfrozen water content in saline permafrost using time domain reflectometry. In Proc. 4th Int. Conf. on Permafrost, Fairbanks, Alaska. Washington, D.C.: National Academy Press, pp. 968-72.

Perreault, P., Shur, Y. 2016. Seasonal thermal insulation to mitigate climate change impacts on foundations in permafrost regions. Cold Regions Science and Technology 132: 7–18.

Phukan, A. 1980. Design of deep foundations in discontinuous permafrost, ASCE Convention and Exposition, Portland, Oregon, 80-122, 1-21.

Phukan, A. 1985. Frozen Ground Engineering. Englewood Cliffs, N.J.: Prentice Hall.

Romanovsky, V.E., and Osterkamp, T.E. 1995. Inter-annual variations of the thermal regime of the active layer and near-surface permafrost in northern Alaska. Permafrost and Periglacial Processes 6(4):313 – 335.

Romanovsky, V.E., and Osterkamp, T.E. 2001. Permafrost: changes and impacts. In: Paepe, R., and Melnikov, V., eds. Permafrost response on economic development,

environmental security and natural resources. Dordrecht, Netherlands: Kluwer Academic Publishers. 297 – 315.

Sanger, F. J. 1969, Foundations of Structures in Cold Regions, U.S. Army Cold Regions Research and Engineering Laboratory Monography III-C4, pp. 91.

Sayles FH, Haines D. 1974. Creep of Frozen Silt and Clay. Cold Regions Research and Engineering Laboratory, Hanover NH; 1974 Jul.

Scott F.S. 1969. The freezing process and mechanics of frozen ground. US Cold Regions Research and Engineering Laboratory. Cold regions science and engineering.

Shur, Y.L., and Jorgenson, M.T. 2007. Patterns of permafrost formation and degradation in relation to climate and ecosystems. Permafrost and Periglacial Processes 18(1):7 – 19.

Smith, S.L., and Burgess, M.M. 2004. Sensitivity of permafrost to climate warming in Canada. Bulletin 579. Ottawa: Geological Survey of Canada, Natural Resources Canada.

Smith, M.W., and Riseborough, D.W. 1996. Permafrost monitoring and detection of climate change. Permafrost and Periglacial Processes 7(4):301 – 309.

Smith, M.W., and Riseborough, D.W. 2002. Climate and the limits of permafrost: A zonal analysis. Permafrost and Periglacial Processes 13(1):1 – 15.

Sture S. 2004. A short course on Computational Geomechanics. University of Colorado at Boulder.

Tice, A.R., Anderson, D.M. and Banin, A. 1976. The Prediction of Unfrozen Water Contents in Frozen Soils from Liquid Limit Determinations. U.S. Army Cold Regions Research and Engineering Laboratory Report CRREL 76-8.

Ting, J.M. 1981. The Creep of Frozen Sands: Qualitative and Quantitative Models. Res. Rep. R81-5. Cambridge, Mass.: Dept. of Civil Engineering, Massachusetts Institute of Technology.

Ting, J.M., R. T. Martin, and C. C. Ladd. 1983. Mechanisms of strength for frozen sand. J. Geotech. Eng. ASCE 109(10):1286-1302.

Tsytovich N.A. 1959. Principles of Geocryology. National Research Council, Tech. Transl. TT 1239, pp. 28-79.

Vialov, S. S. 1959. Rheological properties and bearing capacity of frozen soils. (Russian, translated in 1965.) U.S. Army Corps of Engineers, Cold Regions Research and Engineering Laboratory, Army Translation No. 74, Hanover, NH, 219 p.

Vialov, S. S. 1962. Strength and creep of frozen soils and calculations in ice-soil retaining structures. (Russian, translated in 1965.) U.S. Army Corps of Engineers, Cold Regions Research and Engineering Laboratory, Army Translation No. 76, Hanover, NH, 301 p.

Villeneuve J.R. 2017. Laboratory testing method for adfreeze bond of unsaturated sand on steel piles. M.A.Sc. thesis, University of Ottawa, Ottawa, Canada.

Weaver, J.S. and Morgenstern, N.R. 1981. Pile design in permafrost. Canadian Geotechnical Journal, 18: 357-370.

Weaver, J.S. 1979. Pile foundations in permafrost. Ph.D. diss., Univ. of Alberta, Edmonton, Canada.

Zhang, T. 2005. Influence of the seasonal snow cover on the ground thermal regime: An overview. Reviews of Geophysics 43, RG4002.

Zhang J, Ruan, G., Su K., and Zhang, H. 2016. Estimation on settlement of precast tower footings along the Qinghai–Tibet Power Transmission Line in warm permafrost regions. Cold Regions Science and Technology. 2016 Jan 1; 121:275-81.